

Article

Chemoenzymatic synthesis of proxyphylline enantiomers

Paweł Borowiecki, Daniel Paprocki, Agnieszka Dudzik, and Jan Plenkiewicz

J. Org. Chem., **Just Accepted Manuscript** • DOI: 10.1021/acs.joc.5b01840 • Publication Date (Web): 30 Oct 2015

Downloaded from <http://pubs.acs.org> on November 2, 2015

Just Accepted

"Just Accepted" manuscripts have been peer-reviewed and accepted for publication. They are posted online prior to technical editing, formatting for publication and author proofing. The American Chemical Society provides "Just Accepted" as a free service to the research community to expedite the dissemination of scientific material as soon as possible after acceptance. "Just Accepted" manuscripts appear in full in PDF format accompanied by an HTML abstract. "Just Accepted" manuscripts have been fully peer reviewed, but should not be considered the official version of record. They are accessible to all readers and citable by the Digital Object Identifier (DOI®). "Just Accepted" is an optional service offered to authors. Therefore, the "Just Accepted" Web site may not include all articles that will be published in the journal. After a manuscript is technically edited and formatted, it will be removed from the "Just Accepted" Web site and published as an ASAP article. Note that technical editing may introduce minor changes to the manuscript text and/or graphics which could affect content, and all legal disclaimers and ethical guidelines that apply to the journal pertain. ACS cannot be held responsible for errors or consequences arising from the use of information contained in these "Just Accepted" manuscripts.



ACS Publications

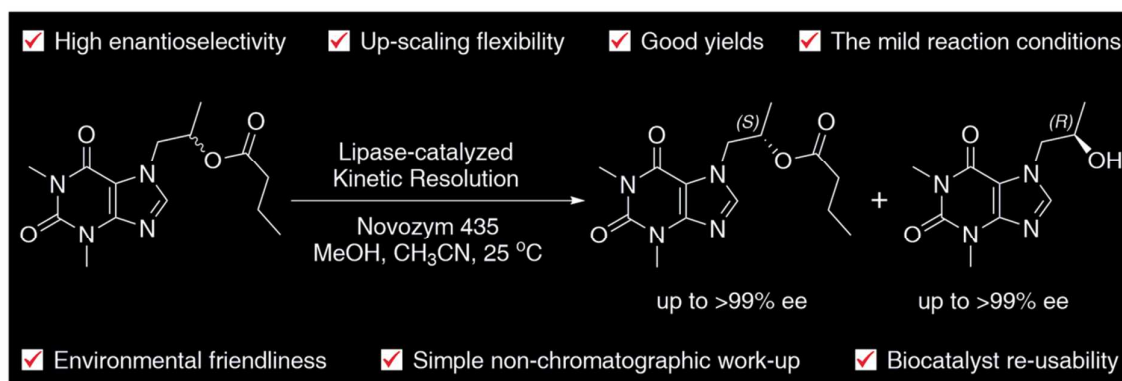
Chemoenzymatic synthesis of proxyphylline enantiomers

Paweł Borowiecki,^{†,*} Daniel Paprocki,[†] Agnieszka Dudzik,[‡] and Jan Pleniewicz[†]

[†] Warsaw University of Technology, Faculty of Chemistry, Institute of Biotechnology, Koszykowa St. 3, 00-664 Warsaw, Poland.

[‡] Jerzy Haber Institute of Catalysis and Surface Chemistry, Polish Academy of Sciences, Niezapominajek St. 8, 30-239 Cracow, Poland.

*Corresponding author: pawel_borowiecki@onet.eu or pborowiecki@ch.pw.edu.pl



ABSTRACT: A novel synthetic route for preparation of proxyphylline enantiomers using a kinetic resolution (KR) procedure as the key step is presented. The reactions were catalyzed by immobilized *Candida antarctica* lipase B in acetonitrile. Three types of reactions were examined: (i) enantioselective transesterification of racemic proxyphylline with vinyl acetate as well as (ii) hydrolysis and (iii) methanolysis of its esters. The influence of reaction conditions on the substrate conversion and enantiomeric purity of the products were investigated. Studies on analytical scale reactions revealed that the titled API enantiomers could be successfully obtained with excellent enantiomeric excess (up to >99% ee). The process was easily conducted on a 5 g scale at 100 g/L. In a preparative-scale reaction, unreacted (S)-(+)-butanoate (97% ee) and (R)-(-)-alcohol (96% ee) were obtained after 2 days in yields of 45% and 46%, respectively. When the reaction time was extended to 6 days (S)-

(+)-butanoate was isolated in >99% ee and acceptable high enantioselectivity ($E=90$). Importantly, the KR's products could be conveniently isolated by exploiting different solubility of the ester/alcohol in acetonitrile at room temperature. In addition, a chiral preference of the CAL-B active site for the *R*-enantiomer was rationalized by *in silico* docking studies.

Key words: Lipase Catalysis; Kinetic Resolution; Proxyphylline; lipase B from *Candida antarctica*, 1,3-Dimethylxanthines, Docking.

1. INTRODUCTION

Chirality is one of the immanent characteristics of nature and plays a key role in metabolic processes as well as in many areas of science and technology.¹ Therefore, synthesis of enantiomerically pure drugs is of prime concern for medicinal chemistry, especially as single stereoisomers of active pharmaceutical ingredients (APIs) can act differently in living systems like human beings or pathogens.² This stems mainly from particular stereoselective interactions at biological receptors (enzymes, hormones etc.), which are build up of chiral molecules, such as amino acids, sugars, and steroids. In order to avert adverse side effects that may pose danger to a patient's life application of chiral pharmaceuticals should have been preceded by thorough biological and clinical evaluations conducted on both racemate and its respective enantiomers.³ Moreover, administering chiral substances as single enantiomers

diminishes the amount of drug to achieve the expected therapeutic effect. For this reason, vast number of racemate separation techniques⁴ including direct preferential crystallization of enantiomeric mixtures (homo- and heterochiral aggregates), fractional crystallization of diastereomeric salts (classical resolution), chromatography on chiral phases, and kinetic resolution mediated by chiral selectors/auxiliaries are essential prerequisites to prepare compounds in enantiomerically pure forms or at least in a very high enantioenrichment. Among aforementioned procedures, especially the protocols employing enzymes as catalysts for kinetic resolution of enantiomers has passed to the canon of synthetic organic chemistry as one of the most elegant and sustainable strategies.

Hydrolases are most commonly employed enzymes, which has received great attention these days.⁵ Among the hydrolytic enzymes, lipases (triacylglycerol ester hydrolases, EC 3.1.1.3) are beyond any doubt the most versatile and practical biocatalysts used in organic chemistry⁶ due to their selectivity in action, wide substrate specificity, commercial availability in both free and immobilized forms, low price, easy handling, high reaction rates, and ability to retain almost full catalytic activity even in nearly anhydrous organic solvents,⁷ in non-conventional media such as neoteric solvents [i.e. ionic liquids (ILs), supercritical carbon dioxide (scCO₂), fluoruous solvents (FSs) and liquid polymers (LPs)]⁸ as well as in solvent-free systems.⁹ Moreover, reactions catalyzed by lipases can be carried out: at high substrate concentration (this prevents misusing of organic solvents and thus improve waste-solvent management), without usage of expensive cofactors, and in ordinary stirred tank reactors (what eliminate restructuring requirements of the conventional chemical apparatus). Lipases can also catalyze transformations of sensitive substrates or complex reactions, for which standard chemical methods are not accessible. Last but not least, it is well documented that lipases are also capable to catalyze asymmetric and non-asymmetric carbon-carbon bond formation what become attractive as very promising alternatives to more traditional synthetic

1
2
3 routes.¹⁰ Apart from improving important bond-forming reactions, so-called ‘lipase
4
5 promiscuity’ can also allow to develop new types of reactivity, which can be exploited to
6
7 provide shorter and more efficient reaction pathways.
8

9
10 Beside the above mentioned characteristics, a number of important developments have
11
12 helped to increase the utility of lipases, including protein engineering,¹¹ protein purification
13
14 methods¹² and immobilization techniques,¹³ which improve enzyme stability, activity, and
15
16 enantioselectivity as well as allow simple catalyst recovery, thereby influencing on the overall
17
18 efficiency of the reactions. In this context, lipases serve as highly valuable and efficient
19
20 catalysts for numerous applications including modification of fats and oils,¹⁴ synthesis of
21
22 pharmaceuticals,¹⁵ agrochemicals,¹⁶ natural products,¹⁷ vitamins,¹⁸ cosmetics,¹⁹ fragrances
23
24 and flavors,²⁰ preparation of modified foods additives,²¹ nutraceuticals,²² detergents,²³
25
26 biodegradable polymers,²⁴ advanced materials²⁵ and biodiesel.²⁶ In addition, the usage of
27
28 lipases in the processing of renewable raw materials,²⁷ in disposing of waste oils and
29
30 lubricants,²⁸ and in biodegradation of toxic xenobiotics²⁹ is also steadily increasing.
31
32
33

34 Although lipases are broadly applicable biocatalysts for enantioselective
35
36 transesterification of structurally different secondary alcohols,³⁰ direct esterification of
37
38 carboxylic acids,³¹ hydrolysis of esters,³² amides,³³ and lactams,³⁴ desymmetrisation of
39
40 prochiral diols/diesters,³⁵ *meso*-1,2-diamines,³⁶ and pentane-1,5-diamines³⁷ as well as
41
42 stereoselective synthesis of *sec*-amines and amino acid derivatives,³⁸ to the best of our
43
44 knowledge, hydrolytic enzymes of this type have not been used toward 1,3-dimethylxanthines
45
46 until now. Moreover, according to the literature, optical resolution of proxyphylline was
47
48 achieved only for its diastereoisomeric camphanates, and carried out by thin-layer
49
50 chromatography (TLC) and fractional crystallization from methanol³⁹ or reversed-phase liquid
51
52 chromatography⁴⁰ mainly for the analytical purposes. In this paper, we present the simple and
53
54 efficient chemoenzymatic synthesis of both proxyphylline enantiomers in a preparative scale.
55
56
57
58
59
60

2. RESULTS AND DISCUSSION

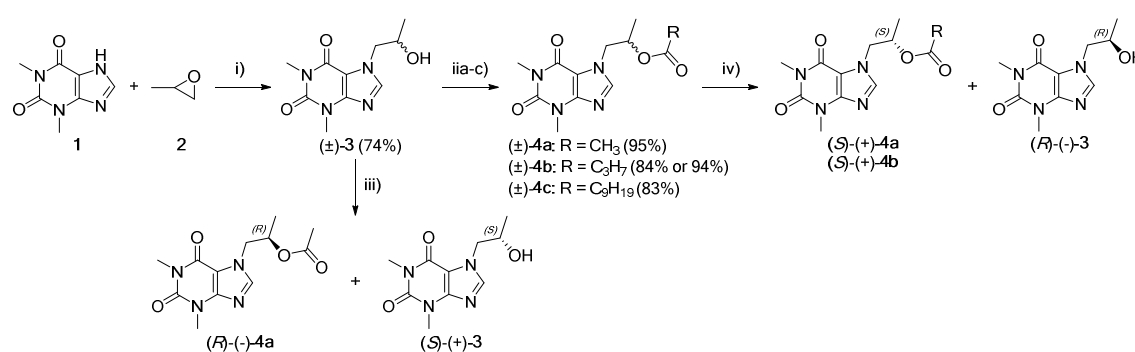
2.1. Synthesis of racemic proxyphylline (\pm)-**3** and its esters (\pm)-**4a-c**

The principal objective of this work was to develop simple and efficient chemoenzymatic procedure for the sustainable synthesis of well-known pharmaceutically valuable compound with cardiac stimulant, vasodilator, and bronchodilator activities – proxyphylline [(\pm)-**3**, 7-(2-hydroxypropyl)-1,3-dimethyl-3,7-dihydro-1*H*-purine-2,6-dione]. In the first step, racemic starting material (\pm)-**3** was synthesized by triethylamine-mediated regioselective ring-opening of propylene oxide **2** with theophylline (**1**, 1,3-dimethyl-7*H*-purine-2,6-dione) in boiling methanol (**Scheme 1**). The reaction proceeded smoothly, and after 4 h, and recrystallization from methanol, the product (\pm)-**3** was prepared in good 74% yield. Interestingly, despite the fact that proxyphylline has been widely used in clinical practice for over 60 years,⁴¹ the nuclear magnetic resonance spectra of (\pm)-**3** has not been reported until now. Next, to obtain racemic esters (\pm)-**4a-c** requested for the preparative enzymatic hydrolysis/methanolysis attempts and robust analytical studies of high performance liquid chromatography (HPLC) separation, the afore-prepared alcohol (\pm)-**3** was treated with acetic anhydride or with the appropriate acyl chloride in dry dichloromethane in the presence of triethylamine and a

catalytic amount of 4-(*N,N*)-dimethylaminopyridine (DMAP). Under 'classical' esterification conditions, esters (\pm)-**4a-c** could be synthesized in the range of high 83-95% yields.

Notably, during the course of this study we have observed quite interesting phenomenon regarding spontaneous polymorphic transformation of one of the racemic esters. Chromatographic purification and subsequent recrystallization of the acetate (\pm)-**4a** from methanol yielded three independent crops of crystalline solids of different, but very narrow melting points range, respectively. At first, we thought that fractions of those products are structurally different, although after analysis it turned out as all these solids are different crystalline structures of proxyphylline acetate (\pm)-**4a**. This feature might be considered very interesting from a pharmaceutical point of view due to its potential influence on drug processing as well as drug quality, safety, and overall performance since the pharmacokinetics, delivery, and bioavailability of biologically active substances is significantly dependent on crystal polymorphism.

Scheme 1. Chemoenzymatic synthesis of both enantiomers of proxyphylline (*S*)-(+)-3** and (*R*)-(-)-**3****



Reagents and conditions: (i) propylene oxide **2** (2 equiv), Et₃N (cat.), MeOH, 4 h at reflux; (iia) Ac₂O (6.5 equiv), DMAP (0.2 equiv), dry CH₂Cl₂, 12 h at rt; (iib) C₃H₇COCl (1.5 equiv) or C₉H₁₉COCl (1.5 equiv), NEt₃ (1.5 equiv), DMAP (0.1 equiv), dry CH₂Cl₂, 12 h at rt; (iic) vinyl butanoate (4.5 equiv), Novozym 435 (5%

w/w), MTBE, 12 h at rt, 1000 rpm; (iii) lipase-catalyzed transesterification: vinyl ester, lipase (20% w/w), solvent, 25 °C, 500 rpm; (iv) lipase-catalyzed hydrolysis/methanolysis: H₂O or Tris-HCl Buffer/MeOH, lipase, solvent, 25 °C, 500 rpm.

Moreover, surprisingly if the alcohol (±)-**3** was treated with vinyl butanoate in the presence of Novozym 435 suspended in methyl *tert*-butyl ether (MTBE), and vigorously stirred (1000 rpm) at room temperature overnight, *O*-butyryl ester (±)-**4b** was afforded in excellent yield (94%) under mild reaction conditions. Although substrate (±)-**3** could not be fully dissolved in neat MTBE, we have found that in the presence of vinyl butyrate solubility of (±)-**3** was considerably enhanced, and thus the esterification process proceeded successfully, providing even better results when compared to ‘classical’ approach. It is important to mention that changing the synthetic strategy toward preparation of (±)-**4b** not only improved the reaction yield, but also helped to ‘greener’ synthesis pathway by eliminating both usage of methylene chloride as the solvent and extraction procedure during the work-up.

2.2. KR of (±)-**3** using lipase-catalyzed transesterification – lipase selection

The development and optimization of a versatile enzymatic methodology is not a simple task, and often lead through many laborious stages including the appropriate lipase selection, effect of enzyme loading, pretreatment, and its conditioning as well as the adequate medium adjustment, proper choice of the acyl group type of donor/acceptor reagent, mutual substrate-to-biocatalyst-to-acyl group donor/acceptor molar/weight ratio, reaction time and temperature etc. Rational planning of enzymatic reaction conditions is critical to meet sustainability criteria.

The water removal process is tedious and expensive at industrial scale. Hence, it is recommended to use synthetic approaches that allow the reactions to be carried out in pure easy-to-evaporate organic solvent or at least in an aqueous-organic two-phase system with the lowest possible water content. The realization of lipase-catalyzed (trans)esterification processes by means of an activated esters (*e.g.* enol esters, trifluoroethyl butyrate, *S*-ethyl thiooctanoate) seems to be the most suitable solution to overcome this problem. Therefore, at the outset of our study, the ability of lipases to catalyze the transesterification of proxyphylline (\pm)-**3** with 11.5-fold molar excess of vinyl acetate as the acetyl transfer reagent in an anhydrous environment was investigated (**Table 1**). The enzymatic KR of the racemate (\pm)-**3** using excess of vinyl acetate as the acetyl transfer reagent and standard protocol was examined in chloroform since surprisingly only this solvent form homogenous solution of the appropriate substrate concentration at 25 °C. None of the other tested solvents including less polar than CHCl₃ [hexane, pentane, toluene, cyclohexane, 2-methyl-2-butanol (*tert*-amyl alcohol)] or more polar [diisopropyl ether, dichloromethane, MTBE, diethyl ether, vinyl acetate, tetrahydrofuran, acetone, acetonitrile, 1,4-dioxane] were suitable for enzymatic acetylation of (\pm)-**3**. Most of the reactions carried out in these solvents resulted in no substrate conversion mainly because of low solubility of (\pm)-**3** in those media. Enzyme screening was attempted using a representative set of 8 lipases isolated from various microorganisms including: *Candida antarctica* B (Novozym 435, Chirazyme L-2, c.-f., C2, Lyo., Chirazyme L-2, c.-f., C3, Lyo.), *Burkholderia cepacia* (Amano PS, Amano PS-IM), *Pseudomonas fluorescens* (Amano AK), *Thermomyces lanuginosus* (Lipozyme TL IM), and *Rhizomucor miehei* (Lipozyme RM IM).

Since the substrate (\pm)-**3** and product (\pm)-**4a** enantiomers do not separate on available Chiralcel OD-H column, determination of the enantiomeric excess values directly from the crude reaction mixture over the course of the process was impossible. Therefore, the progress

of the enzymatic reactions was at first traced by means of non-chiral gas chromatography (GC) in respect to the appropriate calibration curve for quantitative analyses. Next, the reactions were stopped as close to 50% substrate conversion as possible, subsequently isolation by column chromatography was performed, and only then the ee-values were determined by chiral HPLC. In addition, for determination of enantiopurity of title API an extra derivatization procedure of the alcohol into corresponding acetate was required. For that reason, chemical protection of the remaining free hydroxyl functional group was performed by addition of acetic anhydride over catalytic amount of DMAP in dry dichloromethane at room temperature, thus obtaining optically active acetate (*S*)-(+)-**4a** or (*R*)-(-)-**4a** in quantitative yields from (*S*)-(+)-**3** or (*R*)-(-)-**3**, respectively.

Table 1. Lipase screening for the enantioselective *O*-acetylation of (±)-3** under kinetically controlled conditions in CHCl₃**

Entry	Lipase preparation ^a	<i>t</i> [d]	Conv. [%]	ee _s ^b [%]/(config.)	ee _p ^c [%]/(config.)	<i>E</i> ^d
1	Novozym 435	2	53 ^e	59/(<i>S</i>)	52/(<i>R</i>)	6
2	Chirazyme L-2, C-2	2	37 ^e	35/(<i>S</i>)	59/(<i>R</i>)	5
3	Chirazyme L-2, C-3	1	26 ^e	18/(<i>S</i>)	52/(<i>R</i>)	4
4	Amano PS	7	5 ^f	N.D. ^g	N.D. ^g	N.D. ^g
5	Amano PS-IM	7	19 ^e	18/(<i>S</i>)	76/(<i>R</i>)	9
6	Amano AK	1	0	N.D. ^g	N.D. ^g	N.D. ^g
7	Lipozyme TL IM	1	30 ^e	13/(<i>S</i>)	30/(<i>R</i>)	2
8	Lipozyme RM IM	1	0	N.D. ^g	N.D. ^g	N.D. ^g

^a Conditions: (±)-**3** 100 mg, lipase 20 mg, CHCl₃ 1 mL, vinyl acetate 415 mg, 0.5 mL (11.5 equiv), 25 °C, 500 rpm (magnetic stirrer).

^b Determined by chiral HPLC analysis of corresponding alcohol obtained after derivatization of alcohol (*S*)-(+)-**3** into the corresponding acetate (*S*)-(+)-**4a**, which was performed by addition of DMAP and Ac₂O (5 equiv) since direct analysis of (*S*)-(+)-**3** with Chiralcel OD-H column was unsatisfactory.

^c Determined by chiral HPLC analysis by using a Chiralcel OD-H column.

^d Calculated according to Chen *et al.*,⁴² using the equation: $E = \{\ln[(1 - \text{conv.})(1 - \text{ee}_s)]\} / \{\ln[(1 - \text{conv.})(1 + \text{ee}_s)]\}$.

^e Based on GC, for confirmation the % conversion was calculated from the enantiomeric excess of the unreacted alcohol (ee_s) and the product (ee_p) according to the formula $\text{conv.} = \text{ee}_s / (\text{ee}_s + \text{ee}_p)$.

^f Based on gas chromatography (GC).

^g Not determined.

Among the investigated panel of commercially-available preparations, immobilized lipases of a fungal origin such as Novozym 435, Chirazyme L-2, C-2, and Chirazyme L-2, C-3 were established as the most potent biocatalysts for enantioselective transesterification. However, the lipase-catalyzed acetylation of (±)-**3** in CHCl₃ was not successful as the reaction rates and enantioselectivities (*E*=2-9) were far from ideal. Moreover, the enantiomeric

excesses of the desired products [(*S*)-(+)-**3** and (*R*)-(-)-**4a**] were low (18-76% ee), and in consequence evaluation of an enzymatic transesterification of proxyphylline (±)-**3** approach was discontinued. The rest of the lipases (Amano PS, Amano AK, Lipozyme RM IM) proved to be catalytically inactive even after 7 days of proceeding the reactions, while Amano PS-IM and Lipozyme TL IM preparations showed poor selectivity.

2.3. KR of (±)-**4a** using lipase-catalyzed alcoholysis – lipase selection

Since acceptable reaction *E*-factors were impossible to comply with *O*-acetylation procedure (**Table 1**), we have opted to use the reverse process, that is lipase-catalyzed alcoholysis of the acetate (±)-**4a** (**Table 2**). The enzymatic alcoholysis was conducted with methanol as an acetyl-acceptor reagent used in a relatively high ratio to the substrate (±)-**4a** (10 equiv) in spite of well-known fact, that most enzymes are inactivated by low-molecular-weight alcohols, particularly by methanol and ethanol. This stems from propensity of polar/hydrophilic solvents to strip off the essential layer of water molecules from the protein (the structural water), thereby disrupting its native structure responsible for catalysis, and eventually denaturing the enzyme. However, this decision was made intentionally since we have observed positive impact of methanol on the substrate (±)-**4a** solubility. Initially, the same panel of lipases (**Table 1**) was screened as catalysts of asymmetric methanolysis of racemic proxyphylline acetate (±)-**4a** at 25 °C. A detailed survey on selection of the optimal lipase catalyst was carried out using acetonitrile as the solvent. Aliquots of the samples were withdrawn from the reaction mixture at 1 day intervals and the samples were analyzed by GC. Next, the chromatographic purification, and appropriate alcohol derivatization were performed, and the ee-values were measured by means of chiral HPLC. However, preliminary studies gave disappointing results. In most of the studied enzyme systems no reaction was

observed (**Table 2**, entries 4-8) or the lipase-mediated KR proceeded sluggishly achieving barely 2% of the conversion after 24 h (**Table 2**, entry 3). Interestingly, Novozym 435 and Chirazyme L-2, C-2 catalyzed methanolysis of the acetate (\pm)-**4a**, showing promising selective enrichment of the products (**Table 2**, entry 1 and 2). However, the enantiomeric excess values of the liberated alcohol (*R*)-(-)-**3** (72-73% ee) as well as the reaction enantioselectivities (E =16-22) in both cases were poor-to-moderate, and the requested 50% conversions were obtained after as much as 8 days. Although slightly better results in terms of enantioselectivity were obtained in alcoholysis protocol compared to transesterification, still the process proceeded within an unreasonable time-scale. In turn, as the results presented in **Table 2** clearly indicate that (Novozym 435)-catalyzed methanolysis of (\pm)-**4a** yielded unreacted acetate (*S*)-(+)-**4a** with higher optical purity (95% ee) than Chirazyme L-2, C-2 (81% ee), thereby we decided to assess immobilized CAL-B as a potential catalyst for further studies.

Table 2. Lipase screening for the enantioselective methanolysis of (\pm)-4a** under kinetically controlled conditions in CH₃CN**

Entry	Lipase preparation ^a	<i>t</i> [d]	Conv. [%]	ee _s ^b [%]/(config.)	ee _p ^c [%]/(config.)	E^d
1	Novozym 435	8	57 ^e	95/(<i>S</i>)	72/(<i>R</i>)	22
2	Chirazyme L-2, C-2	8	53 ^e	81/(<i>S</i>)	73/(<i>R</i>)	16
3	Chirazyme L-2, C-3	1	2 ^f	N.D. ^g	N.D. ^g	N.D. ^g
4	Amano PS	1	0 ^f	N.D. ^g	N.D. ^g	N.D. ^g
5	Amano PS-IM	1	0 ^f	N.D. ^g	N.D. ^g	N.D. ^g
6	Amano AK	1	0 ^f	N.D. ^g	N.D. ^g	N.D. ^g
7	Lipozyme TL IM	1	0 ^f	N.D. ^g	N.D. ^g	N.D. ^g
8	Lipozyme RM IM	1	0 ^f	N.D. ^g	N.D. ^g	N.D. ^g

^a Conditions: (\pm)-**4a** 100 mg, lipase 20 mg, CH₃CN 1 mL, methanol 114 mg, 0.15 mL (10 equiv), 25 °C, 500 rpm (magnetic stirrer).

^b Determined by chiral HPLC analysis by using a Chiralcel OD-H column.

^c Determined by chiral HPLC analysis of corresponding alcohol obtained after derivatization of alcohol (*R*)-(-)-**3** into the corresponding acetate (*R*)-(-)-**4a**, which was performed by addition of DMAP and Ac₂O (5 equiv) since direct analysis of (*R*)-(-)-**3** with Chiralcel OD-H column was unsatisfactory.

^d Calculated according to Chen *et al.*,⁴² using the equation: $E = \{\ln[(1 - \text{conv.})(1 - \text{ee}_s)]\} / \{\ln[(1 - \text{conv.})(1 + \text{ee}_s)]\}$.

^e Based on GC, for confirmation the % conversion was calculated from the enantiomeric excess of the unreacted ester (ee_s) and the product (ee_p) according to the formula $\text{conv.} = \text{ee}_s / (\text{ee}_s + \text{ee}_p)$.

^f Based on gas chromatography (GC).

^g Not determined.

2.4. KR of (\pm)-**4a** using lipase-catalyzed alcoholysis – the solvent effect

1
2
3 A further important criteria when setting up an enzymatic catalysis with lipases for a given
4 process is the choice of the reaction medium. Selection of an appropriate solvent system (so-
5 called ‘medium engineering’) for a particular enzyme-substrate pair is often very laborious
6 task, but if properly performed it can significantly improve activity, stability, and selectivity
7 of the biocatalyst, and in addition, it may even influence on stereochemical preference of the
8 biocatalyst.⁴³
9
10
11
12
13
14
15

16 This stage of our study has been aimed to optimize the (Novozym 435)-catalyzed KR
17 in alcoholysis of (±)-**4a** with methanol mainly by assessment of the influence of solvent on
18 the conversion rate and stereochemical outcome. For this purpose, an alternative ‘green
19 solvents’ (CH₃CN, 1,4-dioxane, and acetone), a traditional organic solvents with low eco-
20 toxicity (PhCH₃, THF), and chlorinated solvents of a bad reputation (CHCl₃, CH₂Cl₂) were
21 examined as the reaction media. In other commonly-used solvents, well-known for their
22 compatibility with lipases, such as MTBE, diisopropyl ether (DIPE), *n*-hexane and 2-
23 methylbutan-2-ol (*tert*-amyl alcohol, TAA), most of the acetate (±)-**4a** remained in suspension
24 due to poor solubility, and therefore for obvious reasons the reactions were not performed. A
25 screen of media showed that this method also failed to give high enantioselectivities as the
26 best results were obtained still with Novozym 435 suspended in CH₃CN. However, a few
27 observations are noteworthy to comment. Unlikely to common rule that in lipase-catalyzed
28 reactions hydrophobic solvents provide higher reaction rate than hydrophilic one, in our
29 investigations we observed the opposite tendency. This is a surprising result because
30 Novozym 435 was found to retain its catalytic potency in the polar solvents (**Table 3**, entries
31 1-3), showing very similar enantioselectivities (*E*=20-23), while in most of the employed less
32 polar solvents it was inactive toward (±)-**4a** (**Table 3**, entries 4-6). However, the last result
33 (**Table 3**, entry 4) indicates that activity of the lipases might be affected by the solvent
34 without correlation to the log*P*, and therefore other parameters such as solvent–enzyme–
35
36
37
38
39
40
41
42
43
44
45
46
47
48
49
50
51
52
53
54
55
56
57
58
59
60

substrate interactions cannot be ignored, i.e. the accessibility of the substrate to the enzyme active site might be induced by diffusional limitations, changes in protein flexibility or some allosteric regulation controlled by the solvent. Although in the reaction conducted in toluene, unreacted acetate (*S*)-(+)-**4a** was obtained with high 92% ee, however both the degree of conversion and the enantioselectivity were very low indeed. Notably, when comparing both types of the studied lipase-catalyzed reactions, one can see some characteristic behaviour. It turned out that (Novozym 435)-catalyzed transesterification of (\pm)-**3** in chloroform proceeded quite successfully, nevertheless in the case of methanolysis of (\pm)-**4a**, activity of this enzyme was completely lost in water-immiscible chlorinated co-solvents (CHCl_3 or CH_2Cl_2), as the process did not start even after a day. Finally, acetonitrile was found to be the solvent of choice for lipase-mediated methanolysis of (\pm)-**4a**, where other solvents offered decreased rates and worse enantioselectivities.

Table 3. Solvent screening for the enantioselective methanolysis of (\pm)-4a** in the presence of Novozym 435 under kinetically controlled conditions**

Entry	Solvent ^a ($\log P$) ^b	<i>t</i> [d]	Conv. [%]	ee _s ^c [%]/(config.)	ee _p ^d [%]/(config.)	<i>E</i> ^e
1	1,4-Dioxane (-0.31)	10	60 ^f	97/(<i>S</i>)	66/(<i>R</i>)	20
2	CH_3CN (0.17)	8	57 ^f	95/(<i>S</i>)	73/(<i>R</i>)	23
3	Acetone (0.20)	10	54 ^f	89/(<i>S</i>)	75/(<i>R</i>)	21
4	THF (0.40)	1	0 ^g	N.D. ^h	N.D. ^h	N.D. ^h
5	CHCl_3 (1.67)	1	0 ^g	N.D. ^h	N.D. ^h	N.D. ^h
6	CH_2Cl_2 (1.01)	1	0 ^g	N.D. ^h	N.D. ^h	N.D. ^h
7	PhCH_3 (2.52)	14	63 ^f	92/(<i>S</i>)	54/(<i>R</i>)	10

^a Conditions: (\pm)-**4a** 100 mg, lipase 20 mg, solvent 1 mL, methanol 114 mg, 0.15 mL (10 equiv), 25 °C, 500 rpm (magnetic stirrer).

^b Logarithm of the partition coefficient of a given solvent in *n*-octanol-water system according to ChemBioDraw Ultra 13.0 software indications.

^c Determined by chiral HPLC analysis by using a Chiralcel OD-H column.

^d Determined by chiral HPLC analysis of corresponding alcohol obtained after derivatization of alcohol (*R*)-(-)-**3** into the corresponding acetate (*R*)-(-)-**4a**, which was performed by addition of DMAP and Ac_2O (5 equiv) since direct analysis of (*R*)-(-)-**3** with Chiralcel OD-H column was unsatisfactory.

^e Calculated according to Chen *et al.*,⁴² using the equation: $E = \{\ln[(1 - \text{conv.})(1 - \text{ee}_s)]\} / \{\ln[(1 - \text{conv.})(1 + \text{ee}_s)]\}$.

^f Based on GC, for confirmation the % conversion was calculated from the enantiomeric excess of the unreacted ester (ee_s) and the product (ee_p) according to the formula $\text{conv.} = \text{ee}_s / (\text{ee}_s + \text{ee}_p)$.

^g Based on gas chromatography (GC).

^h Not determined.

2.5. Lipase-catalyzed KR of (\pm)-**4a-b** – alcoholysis vs hydrolysis

Adverse results of (±)-**4a** kinetic resolution forced us to explore an alternative asymmetric approach towards synthesis of optically active proxyphylline. In living organisms lipases catalyze hydrolysis of higher fatty acid esters of glycerol, thus fulfill an essential function in metabolism of lipids (e.g. fats and oils) and lipoproteins. As lipases are natural ‘workhorses’ of such chemical transformations in the cells, hence it seems to be reasonable to increase the lipophilicity of proxyphylline (±)-**3** by replacing acetate moiety with longer fatty acyl chains. We envisaged that using butyrate (±)-**4b** or decanoate (±)-**4c** derivatives, which closer mimic natural substrates, the reactions might occur with enhanced enantioselectivity. Unfortunately, as it soon turned out, monitoring of enzymatic reaction with proxyphylline decanoate (±)-**4c** was impossible since GC and HPLC analyses have both failed due to non-volatility of (±)-**4c** in the recommended temperature ranges limits (<260 °C) for the available HP-50+ semipolar column and non-resolvability of (±)-**4c** enantiomers on a Chiralcel OD-H column, respectively. These led us to cease further experiments with (±)-**4c** and hence, we focused on the alcoholysis of acetate (±)-**4a** and butanoate (±)-**4b**. Additionally, the enzymatic KR was examined in water-miscible (monophasic aqueous-organic) solvent systems composed of acetonitrile and water or commercially available 1 M Tris-HCl Buffer, respectively (**Table 4**). The influence of acyl group nature on the course of the ester methanolysis/hydrolysis reaction was examined using 10 equiv of the appropriate acyl acceptor reagent (methanol, H₂O or water which is present in buffer solution) under catalysis of Novozym 435 suspended in CH₃CN as co-solvent, and stirred at 25 °C using a magnetic stirrer (500 rpm). The courses of all the enzymatic reactions were monitored by gas chromatography (GC), arrested deliberately after 8 days, all of the lipase-catalytically resolved products were chromatographically purified, the hydroxyl group of (*R*)-(-)-**3** properly derivatized, and only then their final evolution were subsequently followed by chiral HPLC to compare efficiency of particular methodology. At first glance, the size of acyl group in the examined esters (±)-

4a-b strongly influence the reaction enantioselectivity. The results presented in **Table 4** indicate that KR of butanoate (\pm)-**4b** proceeded with a considerable improvement in the reaction enantioselectivity (E up to 260), furnishing in case of both types of hydrolytic attempts (**Table 4**, entry 5 and 6) very good results in terms of enantiomeric excess of unreacted ester (S)-(+)-**4b** (96-98% ee) as well as the released alcohol (R)-(-)-**3** (94-97% ee). In turn, although (Novozym 435)-catalyzed methanolysis of (\pm)-**4b** was significantly less selective ($E=34$), it turned out that enantioenrichment was remarkably high as the ester (S)-(+)-**4b** was obtained with an excellent enantiomeric excess (>99% ee). Moreover, a comprehensive understanding of the kinetics of lipase-catalyzed reactions prompt us that the potential of methanolysis of (\pm)-**4b** has not been fully evaluated, and an attractive optical purity could be obtained for the opposite enantiomer (R)-(-)-**3** as well. This is fully understandable especially since one realizes that Chen's logarithmic equation⁴² demands very similar levels of conversion, so that the results of E -factor may be reliably compared. As a single experiment cannot be decisive for full estimation of enzymatic performance as well as its potential applicability, it was therefore desirable to compare two types of lipase-mediated transformations – hydrolysis of (\pm)-**4b** in Tris-HCl Buffer as the most enantioselective method, and methanolysis of (\pm)-**4b** as the one, which led to the highest enantiomeric excess of unreacted ester (S)-(+)-**4b**.

Table 4. Examination of (Novozym 435)-catalyzed KR conditions for the enantioselective methanolysis and hydrolysis of (\pm)-4a and (\pm)-4b suspended in CH₃CN after 8 days, respectively

Entry	Compound	Nucleophile	Conv. ^a [%]	ee _s ^b [%]/(config.)	ee _p ^c [%]/(config.)	E^d
1	(±)- 4a	MeOH ^e	57	95/(S)	73/(R)	23
2		H ₂ O ^f	41	64/(S)	94/(R)	63
3		Tris-HCl Buffer ^g	62	52/(S)	84/(R)	8
4	(±)- 4b	MeOH ^h	57	>99/(S)	74/(R)	34
5		H ₂ O ⁱ	51	98/(S)	94/(R)	149
6		Tris-HCl Buffer ^j	50	96/(S)	97/(R)	260

^a Based on GC, for confirmation the % conversion was calculated from the enantiomeric excess of the unreacted ester (ee_s) and the product (ee_p) according to the formula $\text{conv.} = ee_s/(ee_s + ee_p)$.

^b Determined by chiral HPLC analysis by using a Chiralcel OD-H column.

^c Determined by chiral HPLC analysis of corresponding alcohol obtained after derivatization of alcohol (R)-(-)-**3** into the corresponding acetate (R)-(-)-**4a**, which was performed by addition of DMAP and Ac_2O (5 equiv) since direct analysis of (R)-(-)-**3** with Chiralcel OD-H column was unsatisfactory.

^d Calculated according to Chen *et al.*,⁴² using the equation: $E = \{\ln[(1 - \text{conv.})(1 - ee_s)]\} / \{\ln[(1 - \text{conv.})(1 + ee_s)]\}$.

^e Conditions: (\pm)-**4a** 100 mg, lipase 20 mg, CH_3CN 1 mL, MeOH 114 mg, 0.15 mL (10 equiv), 25 °C, 500 rpm (magnetic stirrer).

^f Conditions: (\pm)-**4a** 100 mg, lipase 20 mg, CH_3CN 1 mL, H_2O 64 mg, 0.64 mL (10 equiv), 25 °C, 500 rpm (magnetic stirrer).

^g Conditions: (\pm)-**4a** 100 mg, lipase 20 mg, CH_3CN 1 mL, 1 M Tris-HCl Buffer, pH 7.5 64 mg, 0.64 mL (10 equiv), 25 °C, 500 rpm (magnetic stirrer).

^h Conditions: (\pm)-**4b** 100 mg, lipase 20 mg, CH_3CN 1 mL, MeOH 104 mg, 0.13 mL (10 equiv), 25 °C, 500 rpm (magnetic stirrer).

ⁱ Conditions: (\pm)-**4b** 100 mg, lipase 20 mg, CH_3CN 1 mL, H_2O 58 mg, 0.58 mL (10 equiv), 25 °C, 500 rpm (magnetic stirrer).

^j Conditions: (\pm)-**4b** 100 mg, lipase 20 mg, CH_3CN 1 mL, 1 M Tris-HCl Buffer, pH 7.5 58 mg, 0.58 mL (10 equiv), 25 °C, 500 rpm (magnetic stirrer).

Stimulated by the above results, in the next part of our study, we have examined time dependency on the rate and enantioselectivity of butyrate (\pm)-**4b** methanolysis/hydrolysis under kinetic resolution conditions described in the previous section. For that reason, the conversion degrees of enzymatic reactions were monitored by chiral HPLC over a wide range of reaction times and at various intervals. From the data collected in **Table 5** it become obvious that the methanolysis reaction proceeded more enantioselectively (up to $E=584$) to give both unreacted substrate (S)-(+)-**4b** and product (R)-(-)-**3** in enantiomerically pure form (>99% ee) depending on the moment of process arresting. Another clear advantage of lipase-catalyzed methanolysis over hydrolysis method is easiness of methanol removal by evaporation under reduced pressure or by the extraction, so there is no need to use special water removal procedures.

Table 5. Examination of (Novozym 435)-catalyzed KR time courses for the enantioselective methanolysis and hydrolysis of (\pm)-4b** suspended in CH_3CN , respectively**

Entry	Nucleophile	t [h]	Conv. ^a [%]	ee_s ^b [%]/(config.)	ee_p ^c [%]/(config.)	E^d
1	MeOH ^e	4	46	84/(S)	>99/(R)	532
2		8	47	88/(S)	>99/(R)	584
3		24	48	90/(S)	96/(R)	152
4		48	52	>99/(S)	92/(R)	126
5		72	52	>99/(S)	90/(R)	99
6		96	53	>99/(S)	88/(R)	82
7	Tris-HCl Buffer ^f	24	30	43/(S)	98/(R)	151
8		48	39	63/(S)	98/(R)	190
9		72	45	80/(S)	98/(R)	244
10		96	46	84/(S)	98/(R)	264
11		120	46	85/(S)	98/(R)	270
12		144	47	87/(S)	98/(R)	283

^a Based on GC, for confirmation the % conversion was calculated from the enantiomeric excess of the unreacted ester (ee_s) and the product (ee_p) according to the formula $conv. = ee_s/(ee_s + ee_p)$.

^b Determined by chiral HPLC analysis by using a Chiralcel OD-H column.

^c Determined by chiral HPLC analysis of corresponding alcohol obtained after derivatization of alcohol (R)-(-)-**3** into the corresponding acetate (R)-(-)-**4a**, which was performed by addition of DMAP and Ac_2O (5 equiv) since direct analysis of (R)-(-)-**3** with Chiralcel OD-H column was unsatisfactory.

^d Calculated according to Chen *et al.*,⁴² using the equation: $E = \{\ln[(1 - conv.)(1 - ee_s)]\} / \{\ln[(1 - conv.)(1 + ee_s)]\}$.

^e Conditions: (\pm)-**4b** 100 mg, lipase 20 mg, CH_3CN 1 mL, MeOH 104 mg, 0.13 mL (10 equiv), 25 °C, 500 rpm (magnetic stirrer).

^f Conditions: (\pm)-**4b** 100 mg, lipase 20 mg, CH_3CN 1 mL, 1 M Tris-HCl Buffer, pH 7.5 58 mg, 0.58 mL (10 equiv), 25 °C, 500 rpm (magnetic stirrer).

Analysis of data from kinetic experiments also highlighted that the reaction rates differ substantially in each case. It was noticed that the rate of (Novozym 435)-mediated methanolysis of (\pm)-**4b** was profoundly enhanced compared to hydrolysis, as it reaches ca. 50% conversion after approximately 24 hours, while hydrolysis catalyzed by the same lipase could not achieve this level even after elongation the reaction time over 6 days. Comparing both enantioselective KR courses one can see very characteristic tendency. Although hydrolytic attempt excludes the possibility of achieving enantiopure alcohol (R)-(-)-**3** during the examined time-period, the liberated alcohol has always been afforded with excellent enantiomeric excesses of about 98% (**Table 5**, entries 7-12). In turn, an enantioenrichment increment of the slower reacting enantiomer (S)-(+)-**4b** was negligible, and it finally reached barely 87% ee. In the case of enantioselective hydrolysis of (\pm)-**4b** it was observed that the conversion increased to a certain level (45-47%) after which there was no significant change (**Table 5**, entries 9-12). Note also that it was crucial to follow the kinetics of both lipase-catalyzed reactions very carefully, as it allowed us to determine the appropriate moment to terminate biotransformation of (\pm)-**4b** in order to obtain products of desired enantiomeric purity. Undoubtedly, the experiments revealed classic kinetics of the process that means when lipase-mediated methanolysis process does not exceed 47% conversion it is in favor of enantiopure alcohol (R)-(-)-**3** formation (**Table 5**, entry 1 and 2), while when reaching the conversion above 52% (**Table 5**, entries 4-6) it is beneficial for obtaining unreacted ester (S)-(+)-**4b** as a single enantiomer (>99%). It is noteworthy that maximum enantiomeric excess of

the product (92%) and substrate (>99%) from the same attempt was obtained when the reaction was arrested at conversion of ca. 52% after 2 days of proceeding (**Table 5**, entry 4).

2.6. Preparative-scale lipase-catalyzed KR of (\pm)-**4b** *via* methanolysis

Gratifyingly, an in-depth analysis performed on biotransformation reaction conditions allowed us to obtain strategy fully compatible for the employed xanthine-like derivative (\pm)-**4b**. In the course of our investigation, we found that enzyme-promoted methanolysis unequivocally turned to be the method of choice, as it led to accomplishments of both resolved enantiomers of proxyphylline in high enantiomeric purity, depending on the time and conversion rate. As we developed reliable and robust catalytic system at analytical scale, next we have turned to lipase-catalyzed methanolysis of (\pm)-**4b** under the conditions of kinetic resolution at preparative scale. The commercial CAL-B in immobilized form (Novozym 435) was employed as the catalyst. Crucial advantage of the above-selected lipase preparation is its easy handling and simple isolation of the resolved products. The up-scaling investigations were carried out with 1, 2 and 5 grams of butanoate (\pm)-**4b** respectively using the same optimized reaction procedure as in the analytical scale studies, but obviously with proportionally enlarged reaction stoichiometry (**Table 6**). Unfortunately, we have found that when performing enzymatic processes in a bigger scale, different reaction times were required to obtain both enantiomers of proxyphylline with comparable % ee. The reason of such behavior is unclear for us because we have not met any drawbacks with up-scaling until now. This suggest that such misleading is committed mostly at the stage of the process monitoring. As we mentioned earlier, during this synthesis we could not optimized HPLC analytic method

for reliable tracing of the reaction progress directly from the crude mixture. In this instance, the differences in experimental attempts may be due to the used GC analysis, which is definitely saddled with some error and might appear to be the main source of inaccuracies. Nevertheless, from the results summarized in **Table 6**, it is evident that preparative scale methanolysis of (\pm)-**4b** provided access to both enantiomers of proxyphilline reaching a very high (94-97% ee) to excellent enantiomeric enrichment (98-100% ee).

Table 6. Gram- and multigram-scale enantioselective methanolysis of (\pm)-4b** catalyzed by Novozym 435**

Entry	Scale	<i>t</i> [d]	Conv. ^a [%]	ee _s ^b [%]/Yield ^e (%) / [α] _D ^f	ee _p ^c [%]/Yield ^e (%) / [α] _D ^f	<i>E</i> ^d
1	1 g ^g	1	47	87/95/+42.96 (<i>c</i> 1.35)	98/89/-54.00 (<i>c</i> 1.00)	283
2		3	51	>99/96/+50.36 (<i>c</i> 1.40)	94/90/-50.00 (<i>c</i> 1.00)	170
3	2 g ^h	1	48	88/93/+36.00 (<i>c</i> 1.50)	97/93/-52.38 (<i>c</i> 1.05)	192
4		3	51	>99/94/+45.29 (<i>c</i> 1.70)	95/89/-51.43 (<i>c</i> 1.05)	206
5	5 g ⁱ	2	50	97/90/+41.35 (<i>c</i> 1.85)	96/91/-48.00 (<i>c</i> 1.05)	207
6		6	53	>99/93/+48.89 (<i>c</i> 1.80)	89/94/-47.14 (<i>c</i> 1.00)	90

^a Based on GC, for confirmation the % conversion was calculated from the enantiomeric excess of the unreacted ester (ee_s) and the product (ee_p) according to the formula $\text{conv.} = \text{ee}_s / (\text{ee}_s + \text{ee}_p)$.

^b Determined by chiral HPLC analysis by using a Chiralcel OD-H column.

^c Determined by chiral HPLC analysis of corresponding alcohol obtained after derivatization of alcohol (*R*)-(-)-**3** into the corresponding acetate (*R*)-(-)-**4a**, which was performed by addition of DMAP and Ac₂O (5 equiv) since direct analysis of (*R*)-(-)-**3** with Chiralcel OD-H column was unsatisfactory.

^d Calculated according to Chen *et al.*,⁴² using the equation: $E = \{ \ln[(1 - \text{conv.})(1 - \text{ee}_s)] / \{ \ln[(1 - \text{conv.})(1 + \text{ee}_s)] \} \}$.

^e This value indicates isolated yield after purification step, and is calculated on the basis of the theoretical number of moles arising from conversion rate, relative to theoretical amount, i.e., when 50% conversion is reached, up to the half of the acetate could be obtained.

^f Specific rotation, *c* solution in chloroform, T=27.5 °C.

^g Conditions: (\pm)-**4b** 1 g, lipase 200 mg, CH₃CN 10 mL, MeOH 1.04 g, 1.3 mL (10 equiv), 25 °C, 500 rpm (magnetic stirrer).

^h Conditions: (\pm)-**4b** 2 g, lipase 400 mg, CH₃CN 20 mL, MeOH 2.08 g, 2.6 mL (10 equiv), 25 °C, 500 rpm (magnetic stirrer).

ⁱ Conditions: (\pm)-**4b** 5 g, lipase 1 g, CH₃CN 50 mL, MeOH 5.20 g, 6.6 mL (10 equiv), 25 °C, 500 rpm (magnetic stirrer).

In response to 1 gram reactions, Novozym 435 exhibited excellent enantioselection (*E*=170-283) in the preparative methanolysis of substrate (\pm)-**4b** providing access to the ester

(*S*)-(+)-**4b** with >99% ee and alcohol (*R*)-(-)-**3** with 98% ee (Table 6, entries 1 and 2) depending on time of the process termination and thus the conversion. In the case of 2 gram scale reactions one can see that the results strongly correlated with the previous 1 gram scale attempts (Table 6, entries 1 and 2 vs entries 3 and 4). Hence, if the reaction was arrested after 24 h of proceeding Novozym 435 acted with a high stereopreference in the formation of alcohol (*R*)-(-)-**3** (97% ee) (Table 6, entry 3), whereas the reaction terminated after 3 days yielded unreacted ester (*S*)-(+)-**4b** of >99% ee (Table 6, entry 4). Finally we scaled-up the reaction to 5 grams of racemic substrate (\pm)-**4b** reaching a similar to the presented enantiomeric excess values, but after twice as long reaction times. The lower reaction rate might be due to lower level of enzyme activity regarding the mass transfer coefficient, which in this case mostly depends on the relevant type of the employed reactor. To reach higher conversions in shorter reaction times, the amount of lipase should be doubled and/or the biotransformation of (\pm)-**4b** carried out at higher temperatures. However, industry sector prefers simple reaction systems in which enzyme loading does not exceed 20% (w/w) in relation to substrate due to cost-effectiveness, and elevated temperatures are not willingly applied because of solvent volatility problems, decrease in lipase stereopreference and the limitations in the catalyst reusability. As the preparative scale reactions allowed us to obtain enantiomerically pure ester (*S*)-(+)-**4b** (>99% ee) for acceptable kinetics, and showed potency to be amenable to a large-scale execution, the effects of enzyme concentration and temperature on the activity and enantioselectivity of Novozym 435 for KR of (\pm)-**4b** was intentionally not studied. Examination of the data included in Table 6 reveals that scaling of the reaction up to 1-, 2- and subsequently up to 5 grams of the substrate (\pm)-**4b** gave almost the same isolated yields of recovered ester (*S*)-(+)-**4b** ranging from 90% to 96%, and the formed alcohol (*R*)-(-)-**3** ranging from 89% to 93% with high to excellent enantiomeric excess (87-100% ee) for both resolved enantiomers. In addition, the reusability of the biocatalyst was

tested by conducting the same experiments with the spent catalyst, and we found that Novozym 435 did not show any significant activity loss and erosion of ee even after 3 reuses. This can be recognized as crucial advantage since the lipase was exposed on long and noble contact with stirring bar, which can mechanically crush the immobilization support, resulting in detachment of the enzyme from the carrier as well as on contact with methanol during the reaction, and with chloroform while the filtration and washing procedures were performed. Interestingly, we have found that the resultant alcohol (*R*)-(-)-**3** was precipitated as a crystalline solid during the progress of the reaction. The phenomenon of selective solubility of the alcohol and butanoate in the chosen medium (CH₃CN) potentially increases the utility and practical application of the used synthetic route, as the cumbersome chromatography purification step might be fully excluded after KR procedure. This can be successfully used both in liquid-liquid extractive membrane reactors and/or immobilized enzyme biocatalytic membrane reactors (BMRs) commonly used in industry. The experimental validity of this feature will be verified more deeply in our laboratory in a due course by conducting enzymatic reaction on a larger scale.

2.7. Determination of the lipase stereopreference

Lastly, the absolute configurations of both separated enantiomers [(*S*)-(+)-**4b** and (*R*)-(-)-**3**] were determined by comparison of their optical rotation signs with the data described in the literature. The optical rotation measured for obtained by us samples of enantiomerically pure butyric ester (*S*)-(+)-**4b** (>99% ee) varied from $[\alpha]_{\text{D}}^{27.5} = +45.29$ (*c* 1.70, CHCl₃) to $[\alpha]_{\text{D}}^{27.5} = +50.36$ (*c* 1.40, CHCl₃) depending on the source of their origin (experiment). In turn, the optical rotation determined for the most enantiomerically enriched alcohol (*R*)-(-)-**3** gave $[\alpha]_{\text{D}}^{27.5} = -54.00$ (*c* 1.00, CHCl₃) at 98% ee, which is in accordance with the value given in

literature $[\alpha]_D^{20} = -63.80$ (c 0.42, CHCl_3) at >99% ee for the compound obtained from enantiomerically pure propylene oxide under basic conditions.³⁹ In light of these findings it is clear that the employed Novozym 435 exhibit (*R*)-stereopreference toward racemic ester (\pm)-**4b** since in all of the attempted enzymatic assays it predominantly catalyzed transformation of the (*R*)-enantiomer into the corresponding optically active alcohol (*R*)-(-)-**3** leaving (*S*)-ester almost unreacted. It is reasonable to assume that Novozym 435 manifests the same enantioselectivity with (\pm)-**3** in transesterification reactions, giving the complementary results to lipase-mediated methanolysis in terms of stereochemistry of the resolved enantiomers.

2.8. Docking

There is clearly an urgent need for development of more effective strategies for synthetic methods, hence in depth knowledge of a catalytic behavior of the enzymes as natural asymmetric selectors toward chiral molecules is beneficial. Limited attention has been devoted so far to gain a deeper understanding of the molecular basis of the lipase-catalyzed processes.⁴⁴ Therefore an employment of molecular modeling techniques using docking tools, molecular dynamics (MD) procedures, and quantum mechanics/molecular mechanics (QM/MM) calculations to gain insight into the mechanistic details of lipase catalytic properties should allow rational design of substrates (substrate engineering), reaction conditions (medium engineering), and enzyme (protein engineering) for improved reaction kinetics, yields, and higher enantioselectivity.

In order to rationalize the observed enantioselectivity of (CAL-B)-catalyzed methanolysis of (\pm)-**4b**, we applied an enzyme-substrate docking protocol using non-commercial AutoDock Vina software.⁴⁵ According to the well-known mechanism of action of serine hydrolases,⁴⁶ the employed immobilized CAL-B (Novozym 435) catalyzes the methanolysis of (\pm)-**4b** in the way depicted in **Fig. 1**. In general, the CAL-B active-site

consists of a catalytic triad of Ser105, His224 and Asp187 in which serine is the key aminoacid engaged in biotransformations of xenobiotic substrates, and the remaining two residues are responsible for its nucleophilic activation. The mechanism of (CAL-B)-catalyzed methanolysis of racemic butanoate (\pm)-**4b** involves two steps during which two non-covalent enzyme–substrate complexes [namely, Michaelis complexes (MCCs)] and tetrahedral intermediates (TIs) are formed. In the first step of the reaction, the activated nucleophilic hydroxyl group of the Ser105 attacks the acyl-carbonyl group of the substrate (\pm)-**4b**, thus affording the acyl-enzyme intermediate (acylation step). The formation and collapse of the first tetrahedral intermediate (TI-1) is the rate-determining step of a whole catalytic process. In the second step, the acyl-group of the acylated enzyme (AcCAL-B) reacts with nucleophilic methanol (deacylation step) to form the second tetrahedral intermediate (TI-2), and finally to liberate the enzyme closing the catalytic cycle. In addition, both TIs are stabilized by NH and OH functions in the so-called oxyanion hole of the enzyme, constituted by the Gln106 and Thr40 residues (see **Fig. 1**).

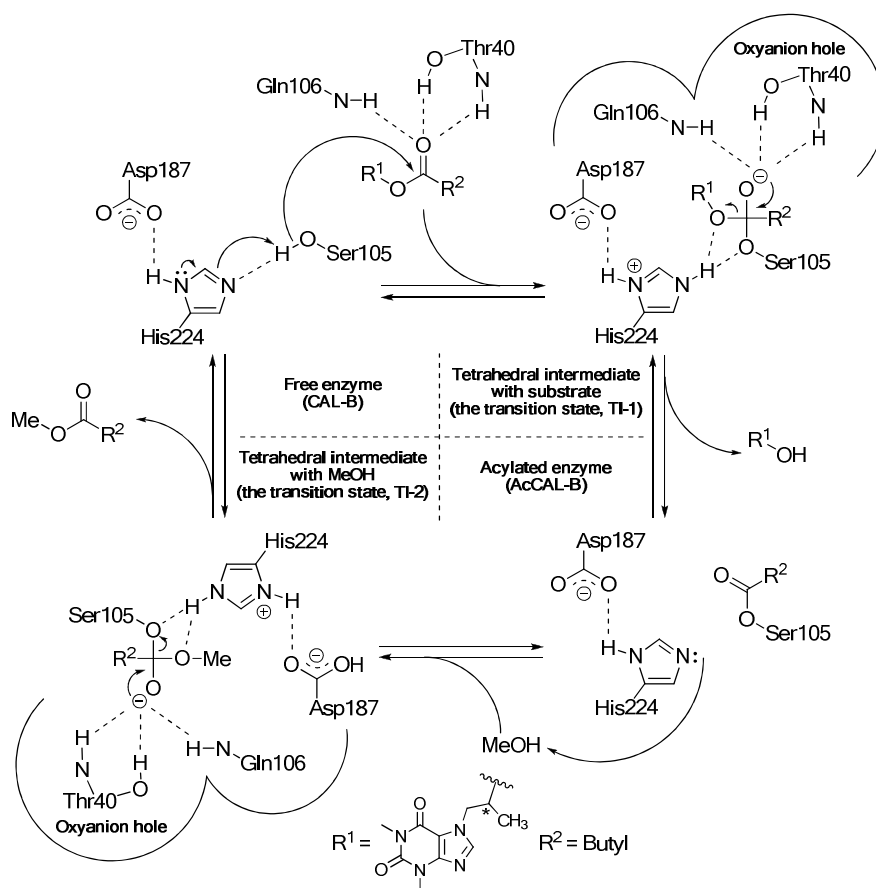


Figure 1. Reaction mechanism (catalytic cycle) of the (CAL-B)-catalyzed methanolysis of (±)-4b.

Moreover, the binding site of CAL-B is composed of two hydrophobic pockets: the large pocket is lined by the respective set of Ile189, Val190, Val154, Leu140, Leu144, Asp134 and Gln157 residues, while the medium pocket is crowded by Trp104, and Leu278–Ala287 helix. The architecture of these pockets force substrate (±)-4b to accommodate within the active-site of CAL-B in two binding modes, namely binding mode I (**Fig. 2 A**) and binding mode II (**Fig. 2 B**), thereby determining the orientation of the substrate molecule toward catalytic triad and the oxyanion hole residues. Because some part of more bulky substrates may extend toward the entrance of the medium-size hydrophobic pocket, the interactions with the solvent in the particular binding mode is obviously relevant as well. For the formation of the enzyme-substrate active complex, the proper location of the substrate

acyl-group against hydroxyl group of the catalytic Ser105 as well as the appropriate interatomic distances, including the catalytic intramolecular hydrogen bonding network between Asp187 and His224 residues, which lead to abstraction of acidic proton from hydroxyl group of Ser105, and thus facilitate the nucleophilic attack (**Fig. 2 C** magenta dashes), must be maintained. Bearing in mind all of the above mentioned requirements, we have taken into account three major criteria when employing docking studies: (i) the distance of the carbon atom of carbonyl group of alkyl side chain of (\pm)-**4b** to the oxygen atom of OH group of the catalytic serine (**Fig. 2 C** orange dashes), (ii) hydrogen bond interactions between the acetyl oxygen of (\pm)-**4b** and the residues of the oxyanion hole (**Fig. 2 C** green dashes), (iii) steric clashes with the enzyme and (iv) other intermolecular polar interactions.

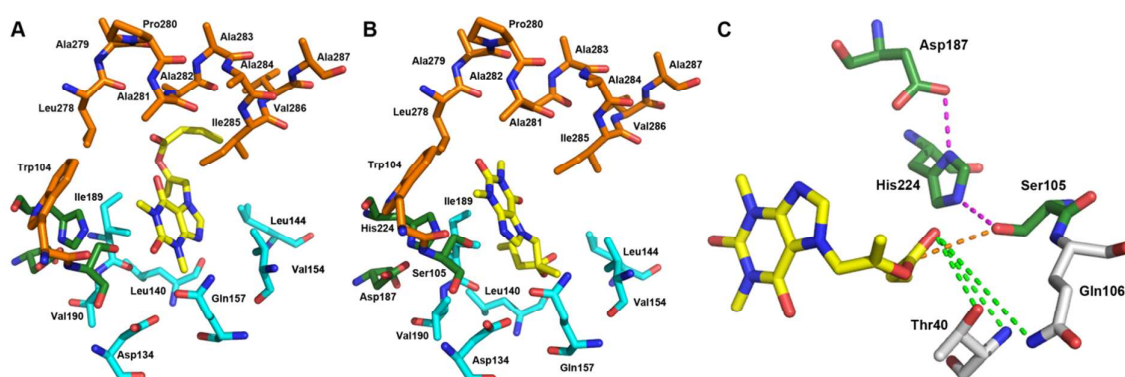


Figure 2. Characteristic binding modes of racemic proxiphylline butanoate (\pm)-**4b** (yellow sticks) in the CAL-B (PDB ID: 1TCA) binding pocket. The active-site geometries of CAL-B with (\pm)-**4b** docked in binding mode I (A) and in binding mode II (B). The binding pocket of CAL-B is constituted by a medium hydrophobic pocket (orange sticks) above the catalytic triad Asp-His-Ser (green sticks) and a large pocket (cyan sticks) below it (A and B). (C) The most important interatomic distances for the catalytic process between substrate (\pm)-**4b**, catalytic triad and the oxyanion hole residues (gray sticks) of the CAL-B are indicated by magenta, green, and orange dashed lines, respectively. The figures were generated using PyMOL.

To disclose the structural factors responsible for higher reactivity of (*R*)-ester than its counterpart in the lipase-catalyzed methanolysis reactions of (\pm)-**4b**, the two enantiomers of

1
2
3 proxyphylline butanoate [(*S*)-(+)-**4b** and (*R*)-(-)-**4b**] were docked separately in the CAL-B
4
5 structure taken from the Protein Data Bank (PDB), with the code 1TCA.⁴⁷ Before docking
6
7 was performed, the target structure of CAL-B was appropriately prepared by deleting all the
8
9 water molecules (including those that were present in the catalytic cavity), and by adding
10
11 polar hydrogen atoms (see Experimental Section). When both enantiomers of (±)-**4b** were
12
13 docked independently into the CAL-B active site, 9 of the most energetically favorable
14
15 binding modes for the ligand-protein complexes for each substrate molecule were generated.
16
17 The results of binding affinity energies (kcal/mol) of the two ligands with the CAL-B enzyme
18
19 are shown in **Tables S2** and **S3**, which are placed in the Supporting Information. Next step
20
21 provided a detail analysis of all the unproductive and productive poses (a stable
22
23 conformations that enable the generation of an acyl-enzyme reactive complexes) selected on
24
25 the basis of the docking conformational search.
26
27
28

29
30 Concerning the two examined enantiomers of substrate (±)-**4b**, it was clear that only
31
32 the *R*-enantiomer displayed a consistent orientation within the CAL-B binding site to obtain
33
34 near attack conformations (NACs) leading to productive complexes (R1 and R2). As shown in
35
36 **Fig. 3**, the fast-reacting (*R*)-enantiomer is embraced inside the hydrophilic pockets of CAL-B
37
38 in position corresponding to the binding mode II postulated above (see **Fig. 2 B**). In this case,
39
40 the large substituent (1,3-dimethylxanthine group) was oriented toward the active-site
41
42 entrance surrounded by hydrophobic Val154, Leu144, Ala141, Leu140 and Ile189 residues,
43
44 meanwhile the acyl moiety was positioned in the stereospecificity acid-binding pocket
45
46 surrounded by Trp104 and Gln157. All the hydrogen bonds required for catalysis were
47
48 spatially arranged, and the distance between Ser105 residue and the carbonyl function of *R*-
49
50 ester was suitable for effective nucleophilic attack. Nevertheless, the selected docking
51
52 conformations of (*R*)-enantiomer (R1 and R2) illustrated in **Fig. 3** are not optimal for lipase-
53
54 catalysis as the distances between carbonyl atom in acyl moiety and the oxygen atom of the
55
56
57
58
59
60

1
2
3 catalytic serine exceed $>4 \text{ \AA}$ (blue dashed lines), and it is too far for rapid nucleophilic attack
4
5 to occur. Importantly, this can explain slow lipase-mediated reaction of the employed racemic
6
7 substrate (\pm)-**4b**. Moreover, the productive conformers of fast-reacting enantiomer are
8
9 efficiently stabilized by polar interactions (magenta dashed lines) between carbonyl oxygen
10
11 atom of *R*-ester and the oxyanion hole Thr40 residue as well as the hydrogen bonds formed
12
13 between carboxylic group of Ile189 and oxygen atom (R1) or nitrogen atom (R2) of xanthine
14
15 ring, respectively.
16
17

18
19 In sharp contrast to the *R*-ester, all the complexes of the slow-reacting (*S*)-enantiomer
20
21 remains at the outer region of the active site, being oriented in space mainly in the binding
22
23 mode I (see Supporting Information), which makes the nucleophilic attack of Ser105
24
25 unfeasible. In the case of the nonpreferential *S*-ester, the docking experiment revealed that
26
27 acyl moiety of the slow-reacting enantiomer is sterically accommodated in the pocket
28
29 surrounded by the subsequent residues Ile189, Ala141, Leu140, and Gln157. This stems
30
31 mainly from van der Waals (vdW) interactions with those surrounding hydrophobic residues
32
33 as well as stabilization of the ligand-protein complexes by electrostatic interactions with the
34
35 nearest neighboring polar atom of the hydrophilic residues Thr40, Gln157, and Ser105. The
36
37 formation of two hydrogen bonds between unsubstituted nitrogen atom of the xanthine moiety
38
39 and the hydroxy side chains of Thr40 and Ser105 residues (S1) pulled the acyl moiety of *S*-
40
41 ester far away from the catalytic triade and the oxyanion hole. Moreover, the analysis of the
42
43 second nonpreferential complex of *S*-ester (S2) revealed that CAL-B could not accommodate
44
45 (*S*)-enantiomer in a catalytically active configuration as easily as (*R*)-enantiomer owing to
46
47 very strong quaternary electrostatic interaction occurred. In this context, the carbonyl group of
48
49 xanthine ring is stabilized through Coulombic interactions with the amide side chain of
50
51 Gln157 as well as intermolecular hydrogen bonding with Thr40 and Ser105, respectively. The
52
53 additional hydrogen bond between the carbonyl oxygen of the ligand acyl moiety and the
54
55
56
57
58
59
60

carboxylic group of Ile189 residue is believed to maintain (*S*)-ester in its ‘uncatalytical accommodation’. The above-mentioned hydrogen bonding network is considered to play an important role in *S*-ligand binding, and thus might impede access to the carbonyl group of the resolved substrate (\pm)-**4b** in the case of the slow-reacting (*S*)-enantiomer.

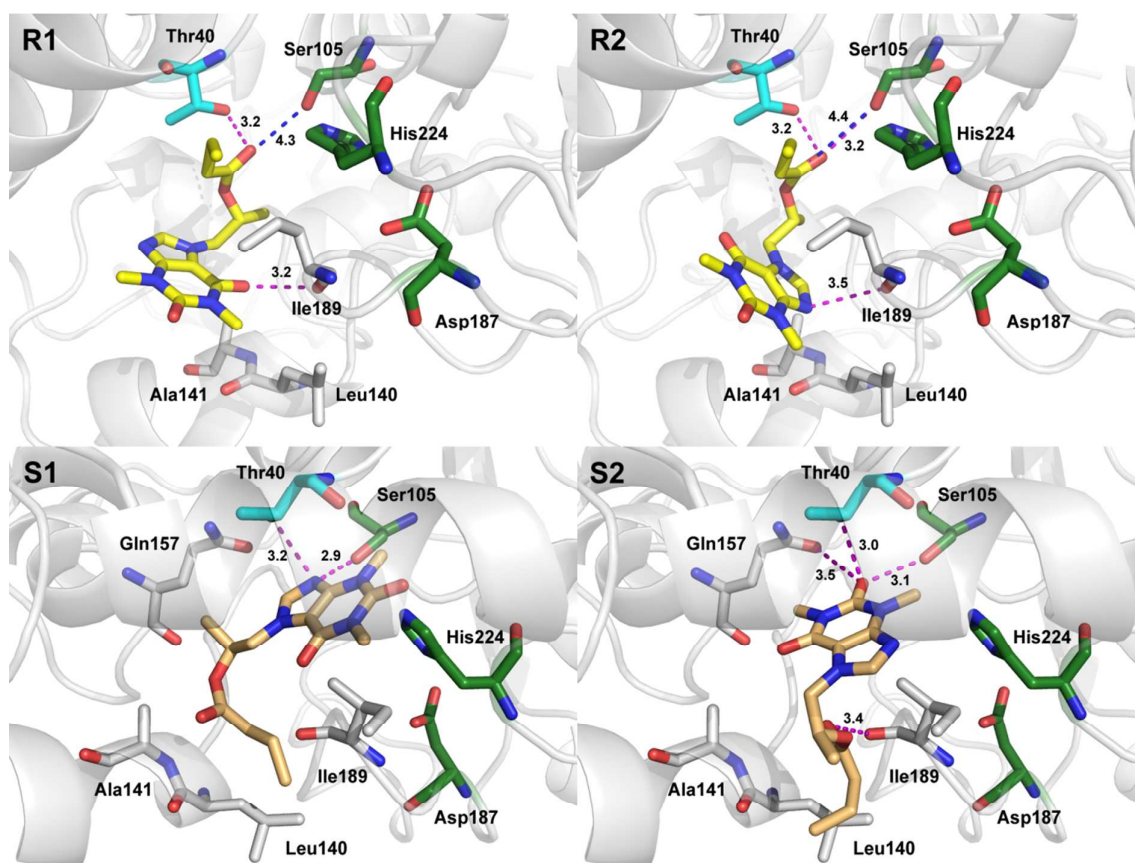


Figure 3. Predominant conformations of (*R*)-(-)-**4b** (yellow sticks) (R1-R2) and (*S*)-(+)-**4b** (lightorange sticks) (S1-S2) in CAL-B (PDB ID: 1TCA) active-site. The residues constituting the catalytic triad (Asp187-His224-Ser105) of CAL-B are shown in green sticks representation. The oxyanionic Thr40 residue is shown in cyan. The rest of the most significant residues contributing to the stabilization of (\pm)-**4b** enantiomers by polar interactions (magenta dashed lines) and by CH-CH van der Waals (vdW) interactions are shown in gray sticks representation. Nitrogen atoms are presented with blue colour, and the oxygen atoms with red colour. The overall enzyme structure is shown as a gray cartoon diagram. The mutual distances between the amino acid residues and ligands atoms are given in Ångström. The different orientation of the enantiomers toward Ser105 and Thr40 is clearly visible. Only the fast-reacting (*R*)-enantiomer (R1 and R2) is near Ser105 (4.3-4.4 Å, the distances are indicated

by blue dashed lines) and additionally stabilized through the formation of hydrogen bonds (magenta dashes) with Thr40 residue (3.2 Å), and Ile189 (3.2-3.5 Å).

In summary, the docking results unambiguously revealed that asymmetric environment in the lipase active-site force stereoselective methanolysis of one of the (±)-**4b** enantiomers since the carbonyl group of the alkyl side chain is situated definitely much closer to the catalytic residues in the *R*-ester complex than in the *S*-ester counterpart. This conformational difference suggests a faster transformation of the *R*-ester over *S*-ester what is certainly correlated to the high *E*-values obtained experimentally. Another evident discriminating factor illustrated in **Fig. 3** is related to the interactions between docked substrate enantiomers and the amino-acid residues of the oxyanion hole. One can see that for the slow-reacting enantiomer, all of the generated conformers are not able to place their potential oxyanion species in the oxyanion hole, with a consequent energy destabilization as compared to the fast-reacting counterpart, where stabilizing hydrogen bonds exists particularly between the oxyanions and Thr40 residue. Based on the results of the molecular docking simulation, we have proved that this method can be successfully used to predict stereopreference of lipases used in biotransformations, and thus it could be helpful in determination of absolute configuration of newly resolved chiral compounds, for which stereochemistry can not be simply assigned by XRD or NMR methodology.

CONCLUSION

In summary, first lipase-catalyzed eco-friendly, facile and scalable approach toward preparation of the single-enantiomer drug proxyphilline was developed. This procedure includes simple kinetic resolution strategy using immobilized lipase B from *Candida antarctica* (Novozym 435). Various enzymatic systems were employed in the critical stage of

the synthetic campaign. Lipase-catalyzed transesterification methodology resulted in unfortunate outcomes, whereas hydrolysis and methanolysis proved very efficient. The influence of enzymatic reaction parameters such as type of lipase, solvent system, reaction time, type of the substrate's acyl group, and scale on stereochemical outcome of kinetic resolution were investigated in detail. To demonstrate the practical viability of this process, Novozym 435 was selected as the most appropriate lipase for preparative use at 1-, 2- and 5-gram scales, respectively. We therefore have devised a straightforward and high-yielding preparation of both enantiomeric forms of proxyphylline with ee's exceeding 89% starting from cheap and renewable material (theophylline) accomplished in a short three-step synthesis. The presented methodology has shown promising potential for use in industry as it was established with many advantages, including high enantioselectivity, up-scaling flexibility, the mild reaction conditions, good yields, and environmental friendliness as well as possibility of simple non-chromatographic work-up. Pleasingly, Novozym 435 could be taken through at least three reaction cycles without a significant loss of activity and enantioselectivity. In addition, a rational explanation of the substrate binding mode was performed by means of Auto Dock Vina software. With docking procedure we have explained the molecular basis of enantioselective resolution of proxyphylline butanoate (\pm)-**4b**. It turned out that only the *R*-enantiomer of (\pm)-**4b** fitted CAL-B binding pocket in conformation of which its acyl group is definitely in a better position to be cleaved by CAL-B than the *S*-ester. On the other hand, the computational analyses revealed that the initiation of the reaction for (*S*)-enantiomer is unfavorable and consequently the *E*-values of the reaction are very high.

EXPERIMENTAL SECTION

General Experimental Methods

Reagents and solvents were purchased from various commercial sources and were used without further purification. Methylene chloride was dried by simply allowing it to stand over activated (oven-roasted in high-vacuum) 3Å molecular sieves [20% mass/volume (m/v) loading of the desiccant] at least for 48 h before use.⁴⁸ All non-aqueous reactions were carried out under oxygen-free argon-protective conditions using flame-dried glassware. Lipase from *Candida antarctica* B [Novozym 435 was purchased from Novo Nordisk A/S (Bagsvaerd, Denmark); Chirazyme L-2, c.-f., C2, Lyo. and Chirazyme L-2, c.-f., C3, Lyo. were both purchased from Roche], lipase from *Burkholderia* (formerly *Pseudomonas*) *cepacia* [Amano PS and Amano PS-IM were purchased from Amano Pharmaceutical Co., Ltd.], lipase from *Pseudomonas fluorescens* [Amano AK was purchased from Amano Pharmaceutical Co., Ltd.], lipase from *Thermomyces lanuginosus* [Lipozyme TL IM was purchased from Novozymes (Bagsvaerd, Denmark)], lipase from *Rhizomucor miehei* [Lipozyme RM IM was purchased from Novozymes A/S (Bagsvaerds, Denmark)]; all commercial formulations of enzymes studied herein were used without any pretreatment. Analytical scale enzymatic reactions were performed in thermo-stated glass vials ($V = 4$ mL) placed in anodized aluminum reaction block (48 position, 19 mm hole depth) dedicated for circular top hot plate stirrer. Melting points, uncorrected, were determined with a commercial apparatus on samples contained in rotating glass capillary tubes open on one side (1.35 mm inner diam. and 80 mm length). Analytical thin-layer chromatography was carried on TLC aluminum plates covered with silica gel of 0.2 mm thickness film containing a fluorescence indicator green 254 nm (F_{254}), and using UV light as a visualizing agent. Preparative separations were carried out by column chromatography using silica gel (230-400 mesh), with grain size 40-63 μm . The chromatographic analyses (GC) were performed with a commercial instrument equipped with a flame ionization detector (FID) and fitted with HP-50+ (30 m) semipolar column (50 %

phenyl–50 % methylpolysiloxane); Helium (2 mL/min) was used as carrier gas; retention times (t_R) are given in minutes under these conditions. The enantiomeric excesses (% ee) of resulting esters and alcohols were determined by HPLC analysis performed on a commercial chromatograph equipped with UV detector and the corresponding commercial Chiralcel OD-H (Diacel) chiral column using mixtures of *n*-hexane/ethanol as mobile phase in the appropriate ratios given in experimental section; the HPLC analyses were executed in an isocratic manner; flow (f) is given in mL/min; racemic alcohols and esters were used as standards; the samples (2 mg) were diluted with mobile phase composed of *n*-hexane/EtOH (1.5 mL; 3:1, v/v). Optical rotations ($[\alpha]$) were measured with commercial polarimeter in a 2 dm long cuvette at 27.5 °C using the sodium D line ($\lambda=589$ nm); the units of the specific rotation $[\alpha]$ are given in (deg×mL)/(g×dm) and calculated from the following equation: $[\alpha] = (100 \times \alpha) / (l \times c)$, where the concentration c is in g/100 mL, α is the measured value, and the path length l is in decimeters; samples were prepared in CHCl₃. UV spectra were measured with spectrometer for the samples prepared in absolute EtOH. ¹H and ¹³C NMR spectra were measured with a commercial spectrometer operating at 400 MHz for ¹H and 100 MHz for ¹³C nuclei; chemical shifts (δ) are given in parts per million (ppm) related to deuterated chloroform (CDCl₃, $\delta = 7.26$) as internal standard; signal multiplicity assignment: s, singlet; d, doublet; t, triplet; q, quartet; m, multiplet; coupling constant (J) are given in hertz (Hz); all of the ¹H and ¹³C NMR spectra were created by non-commercial (freeware) ACD/NMR Processor Academic Edition 12.0. High-resolution mass (HRMS) and Fourier transform mass spectrometry (FTMS) were carried out with electrospray ionization (ESI) using a Q-TOF mass spectrometer. Infrared spectra of neat samples were recorded on a FT-IR spectrophotometer equipped with a attenuated total reflectance (ATR) accessory with a monolithic diamond crystal stage and a pressure clamp; FTIR spectra were recorded in

transmittance mode in the 300-4000 cm^{-1} range, in ambient air at room temperature, with 2 cm^{-1} resolution and accumulation of 32 scans.

Chemical Synthesis

Synthesis of 7-(2-hydroxypropyl)-1,3-dimethyl-3,7-dihydro-1*H*-purine-2,6-dione (\pm)-**3**

The mixture composed of anhydrous theophylline **1** (10 g, 55.51 mmol), propylene oxide **2** (10 g, 0.17 mol, 12 mL), and a catalytic amount of Et_3N (954 mg, 9.44 mmol, 1.3 mL) in MeOH (50 mL) was stirred for 4 h under reflux conditions until the suspension become fully dissolved. Next, half of the volatiles were evaporated and the flask was stored in the fridge for 2 h until the content solidified. Subsequently, the resulting solid was filtered off and washed with cold MeOH (50 mL) yielding desired product (\pm)-**3** as a white crystalline solid (9.77 g, 41 mmol, 74%).

White solid; yield 74%; mp 136-137 $^{\circ}\text{C}$ (MeOH) [lit.⁴¹ 135-136 $^{\circ}\text{C}$ ($\text{EtOH}_{\text{anh.}}$)]; R_f [$\text{CHCl}_3/\text{MeOH}$ (90:10, v/v), silica gel plate] 0.42 or R_f [$\text{CHCl}_3/\text{MeOH}$ (95:5, v/v), silica gel plate] 0.24; $^1\text{H-NMR}$ (CDCl_3 , 400 MHz) δ : 1.24 (d, $J=6.3$ Hz, 3H), 3.15 (br. s., 1H), 3.33 (s, 3H), 3.50 (s, 3H), 4.05 (dd, $J=14.0$, 7.7 Hz, 1H), 4.13-4.23 (m, 1H), 4.44 (dd, $J=13.8$, 2.9 Hz, 1H), 7.60 (s, 1H); $^{13}\text{C-NMR}$ (CDCl_3 , 100 MHz) δ : 20.5, 28.0, 29.8, 53.7, 66.4, 107.0, 142.2, 148.6, 151.3, 155.6; FTMS (ESI-TOF) m/z : $[\text{M}+\text{H}]^+$ Calcd for $\text{C}_{10}\text{H}_{15}\text{N}_4\text{O}_3^+$ 239.11442, Found 239.11361; HRMS (ESI-TOF) m/z : $[\text{M}+\text{H}]^+$ Calcd for $\text{C}_{10}\text{H}_{15}\text{N}_4\text{O}_3^+$ 239.1144, Found 239.1130; HRMS (ESI-TOF) m/z : $[\text{M}+\text{Na}]^+$ Calcd for $\text{C}_{10}\text{H}_{14}\text{N}_4\text{O}_3\text{Na}^+$ 261.0964, Found 261.0955; Anal. Calcd for $\text{C}_{10}\text{H}_{14}\text{N}_4\text{O}_3$: C, 50.41; H, 5.92; N, 23.52. Found: C, 50.42; H, 5.98; N, 23.59; FTIR ν_{max} (neat): 3486.9, 1697.1, 1656.8, 1547.7, 1472.1, 1457.8, 1425.3, 1400.5, 1373.4, 1359.2, 1321.0, 1287.7, 1249.9, 1223.2, 1194.1, 1140.5, 1086.7, 1071.5, 1023.4, 971.2, 940.6, 887.4, 846.7, 759.3, 746.7, 669.0, 619.1, 536.5, 509.3, 476.7, 443.7, 422.3; UV/VIS: λ_{max} = 273 nm (EtOH); GC [230-260 (10 $^{\circ}\text{C}/\text{min}$)]: t_R = 4.80 min or [200-260 (10

°C/min)]: t_R = 6.83 min or [170-260 (3 °C/min)]: t_R = 19.88 min; HPLC [*n*-hexane/EtOH (90:10, v/v); f =0.5 mL/min]: t_R = 40.390 (*S*) and 44.107 (*R*).

Synthesis of racemic 1-(1,3-dimethyl-2,6-dioxo-1,2,3,6-tetrahydro-7*H*-purin-7-yl)propan-2-yl acetate (±)-4a

To the solution of 7-(2-hydroxypropyl)-1,3-dimethyl-3,7-dihydro-1*H*-purine-2,6-dione (proxiphylline) (±)-3 (2 g; 8.39 mmol) in dry CH₂Cl₂ (20 mL), DMAP (205 mg; 1.68 mmol) was added. Next, acetic anhydride (4.28 g, 54.57 mmol, 3.97 mL) was dissolved in dry CH₂Cl₂ (10 mL), and added dropwise to the reaction mixture. Afterward, the resulting mixture was stirred at room temperature for 30 min, and then quenched with water (35 mL). The water phase was extracted with CH₂Cl₂ (3 × 30 mL), and the combined organic layers were washed with saturated NaHCO₃ solution (10 × 100 mL), and dried over Na₂SO₄. The solvent was removed under reduced pressure and the crude product was purified by column chromatography on silica gel using CHCl₃/MeOH (95:5, v/v) as the eluent, evaporated to dryness and subsequently washed with cold MeOH (10 mL) yielding product (±)-4a as a white crystalline solid (2.23 g, 7.96 mmol, 95%).

White solid; yield 95%; mp 51-52.5 °C (crop I, MeOH), mp 84.5-86 °C (crop II, MeOH), mp 92-93.5 °C (crop III, MeOH); R_f [CHCl₃/MeOH (95:5, v/v), silica gel plate] 0.67; ¹H-NMR (CDCl₃, 400 MHz) δ : 1.29 (d, J =6.3 Hz, 3H), 1.97 (s, 3H), 3.38 (s, 3H), 3.57 (s, 3H), 4.23 (dd, J =14.2, 8.1 Hz, 1H), 4.59 (dd, J =14.2, 2.9 Hz, 1H), 5.20-5.29 (m, 1H), 7.54 (s, 1H); ¹³C-NMR (CDCl₃, 100 MHz) δ : 17.2, 21.0, 27.9, 29.8, 50.7, 69.1, 106.9, 141.4, 148.5, 151.5, 155.1, 169.8; FTMS (ESI-TOF) m/z : [M+H]⁺ Calcd for C₁₂H₁₇N₄O₄⁺ 281.12498, Found 281.12420; HRMS (ESI-TOF) m/z : [M+H]⁺ Calcd for C₁₂H₁₇N₄O₄⁺ 281.1250, Found 281.1257; HRMS (ESI-TOF) m/z : [M+Na]⁺ Calcd for C₁₂H₁₆N₄O₄Na⁺ 303.1069, Found 303.1060; Anal. Calcd for C₁₂H₁₆N₄O₄: C, 51.42; H, 5.75; N, 19.99. Found: C, 51.60; H, 5.75;

N, 20.02; FTIR ν_{\max} (neat): 3122.4, 3021.6, 1737.0, 1705.6, 1658.4, 1550.6, 1472.8, 1455.6, 1405.8, 1367.2, 1290.0, 1224.2, 1190.0, 1134.3, 1069.2, 1026.8, 974.2, 961.1, 932.6, 924.5, 894.2, 852.6, 821.8, 759.6, 742.9, 664.3, 640.4, 615.2, 607.8, 509.1, 457.8, 425.6; UV/VIS: λ_{\max} = 273 nm (EtOH); GC [230-260 (10 °C/min)]: t_R = 4.86 min or [170-260 (3 °C/min)]: t_R = 20.46 min; HPLC [*n*-hexane/EtOH (90:10, v/v); f =0.8 mL/min]: t_R = 21.429 (*S*) and 22.908 (*R*) or 21.080 (*S*) and 23.755 (*R*); HPLC [*n*-hexane/EtOH (95:5, v/v); f =0.8 mL/min]: t_R = 38.804 (*S*) and 48.448 (*R*).

Synthesis of racemic 1-(1,3-dimethyl-2,6-dioxo-1,2,3,6-tetrahydro-7*H*-purin-7-yl)propan-2-yl butanoate (±)-4b

Method A: To the solution of 7-(2-hydroxypropyl)-1,3-dimethyl-3,7-dihydro-1*H*-purine-2,6-dione (proxiphylline) (±)-**3** (1.5 g; 6.30 mmol) in dry CH₂Cl₂ (20 mL), Et₃N (955 mg; 9.44 mmol, 1.15 mL) and DMAP (10 mg; 0.13 mmol) were added. The mixture was cooled to 0-5 °C in ice bath. Next, butanoyl chloride (1 g, 9.44 mmol) dissolved in dry CH₂Cl₂ (10 mL) was added dropwise to the reaction mixture. Afterward, the cooling bath was removed, and the resulting mixture was stirred at room temperature overnight, and then quenched with water (35 mL). The water phase was extracted CH₂Cl₂ (3 × 30 mL), and the combined organic layers were washed with saturated solution of NaHCO₃ (2 × 50 mL) and dried over Na₂SO₄. After filtration off the drying agent the solvent was evaporated under reduced pressure, and the crude product was purified by column chromatography on silica gel using CHCl₃/MeOH (95:5, v/v) as the eluent, thus yielding the product (±)-**4b** as yellowish oil (1.63 g, 5.29 mmol, 84%)

Method B: To the solution of 7-(2-hydroxypropyl)-1,3-dimethyl-3,7-dihydro-1*H*-purine-2,6-dione (proxiphylline) (±)-**3** (200 mg; 0.84 mmol) in MTBE (3 mL), Novozym 435 [40 mg, 5% w/w (catalyst/substrate (±)-**3**)], and vinyl butanoate (363 mg; 3.78 mmol) were added in

one portion, and vigorously stirred (1000 rpm) at room temperature overnight. Next, the enzyme was filtered off, washed with MTBE (15 mL), the permeate was partially condensed under reduced pressure, and thus obtained crude product was purified by column chromatography on silica gel using CHCl₃/MeOH (95:5, v/v) as eluent yielding desired ester (±)-**4b** as yellowish oil (252 mg; 0.82 mmol; 97%).

Yellowish oil; yield 94% (corrected on the basis of the NMR assignment); *R_f* [CHCl₃/MeOH (95:5, v/v), silica gel plate] 0.76; ¹H-NMR (CDCl₃, 400 MHz) δ: 0.84 (t, *J*=7.5 Hz, 3H), 1.28 (d, *J*=6.3 Hz, 3H), 1.48-1.59 (m, 2H), 2.18 (td, *J*=7.5, 2.9 Hz, 2H), 3.37 (s, 3H), 3.55 (s, 3H), 4.24 (dd, *J*=14.3, 8.2 Hz, 1H), 4.57 (dd, *J*=14.1, 2.8 Hz, 1H), 5.20-5.30 (m, 1H), 7.52 (s, 1H); ¹³C-NMR (CDCl₃, 100 MHz) δ: 13.5, 17.2, 18.2, 27.9, 29.8, 36.1, 50.7, 68.8, 106.9, 141.4, 148.5, 151.5, 155.1, 172.4; FTMS (ESI-TOF) *m/z*: [M+H]⁺ Calcd for C₁₄H₂₁N₄O₄⁺ 309.15628, Found 309.15556; HRMS (ESI-TOF) *m/z*: [M+H]⁺ Calcd for C₁₄H₂₁N₄O₄⁺ 309.1563, Found 309.1553; HRMS (ESI-TOF) *m/z*: [M+Na]⁺ Calcd for C₁₄H₂₀N₄O₄Na⁺ 331.1382, Found 331.1373; FTIR *v*_{max}(neat): 2964.9, 1735.2, 1701.1, 1650.6, 1604.0, 1546.3, 1473.5, 1456.1, 1426.9, 1407.5, 1374.9, 1288.3, 1252.1, 1228.3, 1172.8, 1133.5, 1087.0, 1066.7, 1024.9, 975.7, 761.1, 747.0, 620.7, 510.5, 474.1, 423.3; UV/VIS: λ_{max} = 274 nm (EtOH); GC [200-260 (10 °C/min)]: *t_R* = 8.48 min; HPLC [*n*-hexane/EtOH (97:3, v/v); *f*=0.4 mL/min]: *t_R* = 77.640 (*S*) and 81.404 (*R*) or 83.323 (*S*) and 87.116 (*R*).

Synthesis of racemic 1-(1,3-dimethyl-2,6-dioxo-1,2,3,6-tetrahydro-7*H*-purin-7-yl)propan-2-yl decanoate (±)-**4c**

To the solution of 7-(2-hydroxypropyl)-1,3-dimethyl-3,7-dihydro-1*H*-purine-2,6-dione (proxiphylline) (±)-**3** (200 mg; 0.84 mmol) in dry CH₂Cl₂ (2 mL), Et₃N (127 mg; 1.26 mmol, 0.13 mL) and DMAP (10 mg; 0.08 mmol) were added in gentle flow of argon. Next, the mixture was cooled to 0-5 °C in ice bath, and decanoyl chloride (240 mg; 1.26 mmol)

dissolved in dry CH_2Cl_2 (1 mL) was added dropwise to the reaction mixture by using a syringe. Afterward, the cooling bath was removed, and the resulting mixture was stirred at room temperature overnight, and then quenched with water (5 mL). The water phase was extracted CH_2Cl_2 (3×5 mL), the combined organic layers were washed with saturated solution of NaHCO_3 (10 mL), brine (10 mL), and dried over Na_2SO_4 . The solvent was evaporated under reduced pressure, and the crude product was purified by preparative-layer chromatography (PLC) using SiO_2 -covered plates and mixture of *n*-hexane/acetone (1.5:1.0, v/v) as the eluent, thus obtaining desired ester (\pm)-**4c** as colorless oil (273 mg; 0.69 mmol; 83%).

Colorless oil; yield 83%; R_f [*n*-hexane/acetone (1.5:1, v/v), silica gel plate] 0.58; $^1\text{H-NMR}$ (CDCl_3 , 400 MHz) δ : 0.85 (t, $J=6.9$ Hz, 3H), 1.16-1.26 (m, 10H), 1.28 (d, $J=6.3$ Hz, 3H), 1.44-1.57 (m, 2H), 2.13-2.17 (m, 2H), 2.20 (td, $J=7.6, 3.6$ Hz, 2H), 3.38 (s, 3H), 3.56 (s, 3H), 4.24 (dd, $J=14.2, 8.1$ Hz, 1H), 4.57 (dd, $J=14.2, 2.9$ Hz, 1H), 5.18-5.32 (m, 1H), 7.51 (s, 1H); $^{13}\text{C-NMR}$ (CDCl_3 , 100 MHz) δ : 14.0, 17.6, 22.5, 24.7, 27.9, 28.9, 29.1, 29.1, 29.3, 29.7, 31.7, 34.2, 50.7, 68.8, 106.8, 141.4, 148.5, 151.4, 155.1, 172.6; FTMS (ESI-TOF) m/z : $[\text{M}+\text{H}]^+$ Calcd for $\text{C}_{20}\text{H}_{33}\text{N}_4\text{O}_4^+$ 393.25018, Found 393.24940; HRMS (ESI-TOF) m/z : $[\text{M}+\text{H}]^+$ Calcd for $\text{C}_{20}\text{H}_{33}\text{N}_4\text{O}_4^+$ 393.2502, Found 393.2490; HRMS (ESI-TOF) m/z : $[\text{M}+\text{Na}]^+$ Calcd for $\text{C}_{20}\text{H}_{32}\text{N}_4\text{O}_4\text{Na}^+$ 415.2321, Found 415.2315; FTIR ν_{max} (neat): 2926.05, 2854.9, 1735.6, 1701.7, 1654.6, 1604.3, 1547.9, 1473.1, 1457.3, 1427.2, 1408.2, 1375.5, 1288.9, 1228.7, 1164.3, 1134.3, 1068.8, 1025.2, 976.5, 761.7, 748.7, 620.6, 509.7, 473.7, 443.6, 423.9; UV/VIS: $\lambda_{\text{max}} = 273$ nm (EtOH); GC analysis failed as (\pm)-**4c** is non-volatile in the recommended temperature ranges limits (<260 °C) recommended for the available column; HPLC analysis also failed as (\pm)-**4c** is not resolvable on a Chiralcel OD-H column.

General procedure for analytical-scale KR of (\pm)-3** using lipase-catalyzed transesterification – enzyme screening**

To the solution of racemic alcohol (\pm)-**3** (100 mg, 0.42 mmol) in CHCl_3 (1 mL) the respective commercial lipase formulation [20 mg, 20% w/w (catalyst/substrate)] and vinyl acetate (415 mg, 4.83 mmol, 0.5 mL) were added in one portion. The reaction mixture was stirred (500 rpm) in a thermo-stated screw-capped test glass vial ($V = 4$ mL) at 25 °C. The progress of the KR was monitored by GC analysis, and after reaching appropriate conversion the reaction was terminated by filtering off the enzyme. After washing the enzyme with CHCl_3 (10 mL), collected chloroform solutions were concentrated under reduced pressure, and the residue was purified by column chromatography on silica gel using mixture of $\text{CHCl}_3/\text{MeOH}$ (95:5, v/v) as the eluent thus affording the respective resolution products [alcohol (*S*)-(+)-**3** and the acetate (*R*)-(-)-**4a**]. Next, to obtain necessary information concerning values of %-conversion, enantiomeric excess (% ee) and enantioselectivity (*E*), the HPLC analyses were performed. For optically active alcohol (*S*)-(+)-**3** an extra derivatization procedure was required (see section *Analysis of enantiomeric purity of (*S*)-(+)-**3** or (*R*)-(-)-**3***). For additional data, see **Table 1**.

General procedure for analytical-scale KR of (\pm)-4a** using lipase-catalyzed alcoholysis – selection of lipase and reaction medium**

Methanol (114 mg, 3.57 mmol, 0.15 mL) and the appropriate lipase [20 mg, 20% w/w (catalyst/substrate)] were added to the solution of racemic acetate (\pm)-**4a** (100 mg, 0.36 mmol) in the respective organic solvent (1 mL), and stirred (500 rpm) in a thermo-stated screw-capped test glass vial ($V = 4$ mL) at 25 °C for the time necessary to achieve good kinetic

resolution (see **Table 2** and **Table 3**). Further manipulations were carried out by analogy with the previously described procedure for the enzyme screening (see section *enzyme screening*).

General procedure for analytical-scale enzymatic KR of (±)-**4b** – alcoholysis vs hydrolysis

Methanol (104 mg, 3.24 mmol, 0.13 mL) or water (58 mg, 3.24 mmol, 0.58 mL) or 1 M Tris-HCl Buffer (58 mg, 3.24 mmol, 0.58 mL, pH 7.5) and Novozym 435 [20 mg, 20% w/w (catalyst/substrate)] were added to the solution of racemic butanoate (±)-**4b** (100 mg, 0.36 mmol) in CH₃CN (1 mL). The reaction mixture was stirred (500 rpm) in a thermo-stated screw-capped test glass vial (*V* = 4 mL) at 25 °C for the necessary time to achieve good kinetic resolution (see **Table 4** and **Table 5**). For the hydrolytic attempts, after enzyme removal and washing the filter cake with CHCl₃ (10 mL), the permeate was additionally dried over Na₂SO₄, filtered off, and evaporated to dryness under reduced pressure. The residue was separated by column chromatography on silica gel using CHCl₃/MeOH (95:5, v/v) as the eluent yielding optically active products [ester (*S*)-(+)-**4b** and alcohol (*R*)-(-)-**3**].

General procedure for 2-gram scale (Novozym 435)-catalyzed KR of (±)-**4b** by methanolysis

The reaction mixture containing racemic ester (±)-**4b** (2 g, 6.49 mmol), CH₃CN (20 mL), MeOH (2.08 g, 64.87 mmol, 2.63 mL), and Novozym 435 [400 mg, 20% w/w (catalyst/substrate (±)-**3**)] was stirred (500 rpm, IKA RCT basic) in round-bottomed flask (50 mL) at 25 °C for the appropriate time (see **Table 6**). The reaction was followed by GC analysis until ca. 50% substrate conversion was reached. The enzyme was then removed by filtration and washed with CHCl₃ (50 mL). Next, the combined solutions were evaporated under reduced pressure, and the crude products were purified by column chromatography on

silica gel using gradient of CHCl₃/MeOH (95:5, 90:10, v/v) mixture as the eluent, affording the corresponding optically active butanoate (*S*)-(+)-**4b** (93-94% yield, 88-100% ee) and alcohol (*R*)-(-)-**3** (89-93% yield, 95-97% ee). The given isolated yields are based on the maximum amount which can be stoichiometrically obtained, that is, on a half amount of (±)-**4b** used in the case of the reaction stopped at 50% conversion. The results of enzymatic KR for 1- and 2-gram scale, including products optical rotation values, are collected in **Table 6**.

General procedure for 5-gram scale (Novozym 435)-catalyzed KR of (±)-4b** by methanolysis**

The reaction mixture containing racemic ester (±)-**4b** (5 g, 16.22 mmol), CH₃CN (50 mL), MeOH (5.20 g, 0.16 mol, 6.60 mL), and Novozym 435 [1 g, 20% w/w (catalyst/substrate (±)-**3**)] was stirred (500 rpm) in round-bottomed flask (250 mL) equipped with a Teflon-coated magnetic stirring bar (20 × 5 mm, 2 g) at 25 °C for the appropriate time (see **Table 6**). The course of the reaction was followed by GC analysis until ca. 50% conversion was reached. Enzymatic KR was stopped by filtering off the enzyme together with the precipitated alcohol product (*R*)-(-)-**3**. The permeate containing dissolved unreacted butanoate (*S*)-(+)-**4b** and residues of the formed alcohol (*R*)-(-)-**3** was partially concentrated in vacuo, left in refrigerator for 3 h, and afterwards, the resulting white precipitate of the alcohol was collected by filtration. The filtrate was again concentrated, and passed through short silica pad eluting with mixture of CHCl₃/MeOH (80:20, v/v) to obtain optically active butanoate (*S*)-(+)-**4b** (90-93% yield, from 97% ee to >99% ee). The alcohol (*R*)-(-)-**3** was also recovered from the filter cake (enzyme + precipitate) by washing it with CHCl₃ (50 mL), evaporating of the solvent to dryness, adding portion of MeOH, and finally, leaving the content in the fridge until white precipitate of the alcohol was formed. Both obtained crops were collected, and purified by recrystallization from MeOH to give enantiomerically enriched alcohols (*R*)-(-)-**3** (91-94%

yield, 89-96% ee). The experimental conditions and the results of enzymatic KR reactions for 5-gram scale, including products optical rotation values, are collected in **Table 6**. Physical, spectroscopic and analytical data are identical with the corresponding racemic standard compounds.

Determination of enantiomeric purity of (*S*)-(+)-**3** or (*R*)-(-)-**3**

The enantiomeric excess (% ee) of the alcohol enantiomers (*S*)-(+)-**3** or (*R*)-(-)-**3** (20 mg, 0.08 mmol) was determined by HPLC on a chiral phase after derivatization to the corresponding acetate (*S*)-(+)-**4a** or (*R*)-(-)-**4a**, which was performed by addition of an catalytic amount of DMAP (3 mg) and a 5-fold excess of acetic anhydride (43 mg, 0.42 mmol, 40 μ L) dissolved in CH₂Cl₂ (0.4 mL) and vigorous stirring for 15 min at ambient temperature. Next, portion of CH₂Cl₂ (0.8 mL) was added and washed with saturated NaHCO₃ (4 \times 1 mL) until effervescence ceased. Subsequently, the organic phase was separated, dried over mixture of anhydrous K₂CO₃, Na₂SO₄ and MgSO₄, and after filtration of the drying agents the solvent residual was removed under vacuum. The respective crude acetate was subsequently dissolved in mixture of *n*-hexane/EtOH (1.5 mL, 3:1, v/v) and directly injected without further cleanup. An alternative method of the sample purification was based on short column chromatography on silica gel in the eluent system containing mixture of CHCl₃-MeOH (90:10, v/v).

Docking studies

Computer molecular dynamics simulations (docking studies) to determine favorable ligand binding geometries for the substrates were carried out using AutoDock Vina vs. 1.1.2 program for Windows (<http://autodock.scripps.edu/>).⁴⁵ Ligand molecules were prepared with ChemAxon MarvinSketch vs. 14.9.1.0 (<http://www.chemaxon.com/marvin/>) and saved as

.PDB or .mol2 files, respectively. Gasteiger partial charges were calculated with AutoDock Tools vs. 1.5.6 (ADT, S3 <http://mgltools.scripps.edu/>),⁴⁹ and the final ligand files were prepared in PDBQT format. The crystallographic structures of lipase from *Candida antarctica* B (PDB code 1TCA)⁴⁷ was downloaded from Brookhaven RCSB Protein Data Bank (PDB, <http://www.rcsb.org/pdb/>). Crude protein .pdb file was prepared by UCSF Chimera vs. 1.9 package (<http://www.cgl.ucsf.edu/chimera/>).⁵⁰ All nonstandard (non-protein) molecules including the two sugar units (NAG) and 286 crystal waters were removed, the polar hydrogen atoms were added and Gasteiger charges were calculated with AutoDock Tools 1.5.6 package.⁴⁵ With use of AutoGrid, a searching grid box was set in the appropriate size before docking. The box center was set at catalytic Ser105 of CAL-B. Docking was performed in 40×40×40 units grid box centered on the enzyme active-site (center_x = -3.144; center_y = 21.093; center_z = 12.736) with the grid spacing of 0.325 Å. Each docking was performed with an exhaustiveness level of 48. For each ligand molecule 100 independent runs were performed, using Lamarckian genetic algorithm (GA), with at most 106 energy evaluations and maximum number of generations of >27 000 Å³ (the search space volume). The remaining GA parameters were set as default. The docking configurations of each ligand were ranked on the basis of free binding energy (kcal/mol). The best 9 poses (modes) were selected according to AutoDock Vina scoring functions mainly based on binding energies, and show mutual affinity (kcal/mol). Each selected binding mode was manually inspected in order to select only productive conformations where the substrate assumes a Near Attack Conformation (NAC) compatible with the attack of the catalytic serine (Ser105) to the carbon atom of the acyl group of the ligand. The molecular modeling treated the two isomers (*R* and *S*) independently, and the docking procedure used both isomers for each compound. The docked ligand conformations and the subsequent analysis of intermolecular interactions in CAL-B active-site were performed with The PyMOL Molecular Graphics System software,

Version 1.3 Schrödinger, LLC (<https://www.pymol.org/>). For docking scoring see the Supporting Information.

ASSOCIATED CONTENT

Supporting Information

Copies of ^1H NMR, ^{13}C NMR, HRMS, FTMS, IR, UV/VIS spectra and HPLC, GC chromatograms of all compounds as well as docking scoring. This material is available free of charge via the Internet at <http://pubs.acs.org>.

AUTHOR INFORMATION

Corresponding Author

pawel_borowiecki@onet.eu or pborowiecki@ch.pw.edu.pl

Notes

The authors declare no competing financial interests.

ACKNOWLEDGMENTS

Author wish to acknowledge National Science Center of Poland (No. 2014/13/N/ST5/01589) for the financial support. This work was partially supported by the Warsaw University of Technology, Faculty of Chemistry.

REFERENCES

- (1) (a) Agranat, I.; Caner, H.; Caldwell, *J. Nat. Rev. Drug Disc.* **2002**, *1*, 753–768. (b) Caldwell, *J. Hum. Psychopharmacol. Clin. Exp.* **2001**, *16*, 67–71.

- (2) (a) Kasprzyk-Hordern, B. *Chem. Soc. Rev.* **2010**, *39*, 4466–4503. (b) Mentel, M.; Blankenfeldt, W.; Breinbauer, R. *Angew. Chem., Int. Ed.* **2009**, *48*, 9084–9087. (c) Carey, J. S.; Laffan, D.; Thomson, C.; Williams, M. T. *Org. Biomol. Chem.* **2006**, *4*, 2337–2347.
- (3) Branch, S.; Subramanian, G. In *International Regulation of Chiral Drugs. Chiral Separation Techniques. A Practical Approach*; Subramanian, G., Branch, S., (Eds.); Wiley-VCH: Weinheim, 2001; pp 319–342.
- (4) (a) Lorenz, H.; Seidel-Morgenstern, A. *Angew. Chem. Int. Ed. Engl.* **2014**, *53*, 1218–12150. (b) Tzschucke, C. C.; Markert, C.; Bannwarth, W.; Roller, S.; Hebel, A.; Haag, R. *Angew. Chem. Int. Ed.* **2002**, *41*, 3964–4000.
- (5) Holmquist, M. *Curr. Protein Peptide Sci.* **2000**, *1*, 209–235.
- (6) (a) Gupta, R.; Kumari, A.; Syal, P.; Singh, Y. *Prog. Lipid Res.* **2015**, *57*, 40–54. (b) Stergiou, P. Y.; Foukis, A.; Filippou, M.; Koukouritaki, M.; Parapouli, M.; Theodorou, L. G.; Hatziloukas, E.; Afendra, A.; Pandey, A.; Papamichael, E. M. *Biotechnol. Adv.* **2013**, *31*, 1846–1859. (c) Ghanem, A. *Tetrahedron* **2007**, *63*, 1721–1754.
- (7) (a) Salihu, A.; Alam, M. Z. *Process Biochem.* **2015**, *50*, 86–96. (b) Adlercreutz, P. *Chem. Soc. Rev.* **2013**, *42*, 6406–6436. (c) Zaks, A.; Klivanov, A. M. *Proc. Natl. Acad. Sci.* **1985**, *82*, 3192–3196. (d) Sym, E. A. *Biochem. J.* **1936**, *30*, 609–617.
- (8) (a) Rodrigues, J. V.; Ruivo, D.; Rodríguez, A.; Deive, F. J.; Esperança, J. M. S. S.; Marrucho, I. M.; Gomes, C. M.; Rebelo, L. P. N. *Green Chem.* **2014**, *16*, 4520–4523. (b)

- De Diego, T.; Manjón, A.; Lozano, P.; Vaultier, M.; Iborra, J. L. *Green Chem.* **2011**, *13*, 444–451. (c) Filice, M.; Guisan, J. M.; Palomo, J. M. *Green Chem.* **2010**, *12*, 1365–1369.
- (9) (a) Corici, L.; Pellis, A.; Ferrario, V.; Ebert, C.; Cantone, S.; Gardossi, L. *Adv. Synth. Catal.* **2015**, *357*, 1763–1774. (b) El-Boulifi, N.; Ashari, S. E.; Serrano, M.; Aracil, J.; Martinez, M. *Enzyme Microb. Technol.* **2014**, *55*, 128–132. (c) Pyo, S.-H.; Persson, P.; Lundmark, S.; Hatti-Kaul, R. *Green Chem.* **2011**, *13*, 976–982.
- (10) (a) Guan, Z.; Li, L.-Y.; He, Y.-H. *RSC Adv.* **2015**, *5*, 16801–16814. (b) Zhang, Y.; Vongvilai, P.; Sakulsombat, M.; Fischer, A.; Ramström, O. *Adv. Synth. Catal.* **2014**, *356*, 987–992. (c) Kapoor, M.; Gupta, M. N. *Process Biochem.* **2012**, *47*, 555–569.
- (11) (a) Wu, Q.; Soni, P.; Reetz, M. T. *J. Am. Chem. Soc.* **2013**, *135*, 1872–1881. (b) Reetz, M. T. *J. Am. Chem. Soc.* **2013**, *135*, 12480–12496. (c) Ema, T.; Nakano, Y.; Yoshida, D.; Kamata, S.; Sakai, T. *Org. Biomol. Chem.* **2012**, *10*, 6299–6308. (d) Brundiek, H. B.; Evitt, A. S.; Kourist, R.; Bornscheuer, U. T. *Angew. Chem.* **2012**, *51*, 412–414.
- (12) (a) Barbosa, O.; Ortiz, C.; Berenguer-Murcia, A.; Torres, R.; Rodrigues, R. C.; Fernandez-Lafuente, R. *Biotechnol. Adv.* **2015**, *33*, 435–456. (b) Souza, R. L.; Lima, R. A.; Coutinho, J. A. P.; Soares, C. M. F.; Lima, Á. S. *Sep. Pur. Technol.* **2015**, *In Press*. (c) Souza, R. L.; Lima, R. A.; Coutinho, J. A. P.; Soares, C. M. F.; Lima, Á. S. *Process Biochem.* **2015**, *50*, 1459–1467.
- (13) (a) Zhao, D.; Peng, C.; Zhou, J. *Phys. Chem. Chem. Phys.* **2015**, *17*, 840–850. (b) Nascimento, M. d. G.; da Silva, J. M. R.; da Silva, J. C.; Alves, M. M. *J. Mol. Catal. B:*

Enzym. **2015**, *112*, 1–8. (c) Esmaeilnejad-Ahranjani, P.; Kazemeini, M.; Singh, G.; Arpanaei, A. *RSC Adv.* **2015**, *5*, 33313–33327. (d) Adlercreutz, P. *Chem. Soc. Rev.* **2013**, *42*, 6406–6436.

(14) (a) Su, E.; Wei, D. *J. Agric. Food Chem.* **2014**, *62*, 6375–6381. (b) Qin, X. L.; Yang, B.; Huang, H. H.; Wang, Y. H. *J. Agric. Food Chem.* **2012**, *60*, 2377–2384. (c) Teichert, S. A.; Akoh, C. C. *J. Agric. Food Chem.* **2011**, *59*, 9588–9595.

(15) (a) Hertzberg, R.; Monreal Santiago, G.; Moberg, C. *J. Org. Chem.* **2015**, *80*, 2937–2941. (b) Dwivedee, B. P.; Ghosh, S.; Bhaumik, J.; Banoth, L.; Chand Banerjee, U. *RSC Adv.* **2015**, *5*, 15850–15860. (c) Ramesh, P.; Harini, T.; Fadnavis, N. W. *Org. Proc. Res. Dev.* **2015**, *19*, 296–301. (d) Fonseca, T. d. S.; Silva, M. R. d.; de Oliveira, M. d. C. F.; Lemos, T. L. G. d.; Marques, R. d. A.; de Mattos, M. C. *Appl. Catal. A: Gen.* **2015**, *492*, 76–82. (e) Sayin, S.; Akoz, E.; Yilmaz, M. *Org. Biomol. Chem.* **2014**, *12*, 6634–6642. (f) Borowiecki, P.; Paprocki, D.; Dranka, M. *Beilstein J. Org. Chem.* **2014**, *10*, 3038–3055.

(16) (a) Krumlinde, P.; Bogár, K.; Bäckvall, J. E. *J. Org. Chem.* **2009**, *74*, 7407–7410. (b) Zhou, R.; Xu, J.-H. *Biochem. Eng. J.* **2005**, *23*, 11–15. (c) Cheng, Y.-C.; Tsai, S.-W. *Tetrahedron: Asymmetry* **2004**, *15*, 2917–2920.

(17) (a) Lu, P.; Herrmann, A. T.; Zakarian, A. *J. Org. Chem.* **2015**, *80*, 7581–7589; (b) Beretta, R.; Giambelli Gallotti, M.; Penne, U.; Porta, A.; Gil Romero, J. F.; Zannoni, G.; Vidari, G. *J. Org. Chem.* **2015**, *80*, 1601–1609. (c) Risi, R. M.; Maza, A. M.; Burke, S. D. *J. Org. Chem.* **2015**, *80*, 204–216. (d) Yamamoto, H.; Takagi, Y.; Oshiro, T.;

Mitsuyama, T.; Sasaki, I.; Yamasaki, N.; Yamada, A.; Kenmoku, H.; Matsuo, Y.; Kasai, Y.; Imagawa, H. *J. Org. Chem.* **2014**, *79*, 8850–8855.

(18) (a) Wei, C.; Fu, X.-F.; Wang, Z.; Yu, X.-J.; Zhang, Y.-J.; Zheng, J.-Y. *J. Mol. Catal. B: Enzym.* **2014**, *106*, 90–94. (b) Torres, P.; Kunamneni, A.; Ballesteros, A.; Plou, F. J. *The Open Food Sci. J.* **2008**, *2*, 1–9. (c) Torres, P.; Reyes-Duarte, D.; López-Cortés, N.; Ferrer, M.; Ballesteros, A.; Plou, F. J. *Process Biochem.* **2008**, *43*, 145–153.

(19) Ansorge-Schumacher, M. B.; Thum, O. *Chem. Soc. Rev.* **2013**, *42*, 6475–6490.

(20) (a) Martins, A. B.; da Silva, A. M.; Schein, M. F.; Garcia-Galan, C.; Záchia Ayub, M. A.; Fernandez-Lafuente, R.; Rodrigues, R. C. *J. Mol. Catal. B: Enzym.* **2014**, *105*, 18–25. (b) Lozano, P.; Bernal, J. M.; Navarro, A. *Green Chem.* **2012**, *14*, 3026–3033. (c) Brenna, E.; Fuganti, C.; Gatti, F. G.; Serra, S. *Chem. Rev.* **2011**, *111*, 4036–4072.

(21) (a) Cao, M.; Fonseca, L. M.; Schoenfuss, T. C.; Rankin, S. A. *J. Agric. Food Chem.* **2014**, *62*, 5726–5733. (b) Okino-Delgado, C. H.; Fleuri, L. F. *Food Chem.* **2014**, *163*, 103–107. (c) Ferreira-Dias, S.; Sandoval, G.; Plou, F.; Valero, F. *Electronic J. Biotechnol.* **2013**, *16*, 3–5.

(22) (a) Wang, J.; Wang, S.; Li, Z.; Gu, S.; Wu, X.; Wu, F. *J. Mol. Catal. B: Enzym.* **2015**, *111*, 21–28. (b) Zheng, M.-M.; Wang, L.; Huang, F.-H.; Guo, P.-M.; Wei, F.; Deng, Q.-C.; Zheng, C.; Wan, C.-Y. *J. Mol. Catal. B: Enzym.* **2013**, *95*, 82–88. (c) Sorour, N.; Karboune, S.; Saint-Louis, R.; Kermasha, S. *J. Biotechnol.* **2012**, *158*, 128–136.

- (23) (a) Weerasooriya, M. K. B.; Kumarasinghe, A. A. N. *Indian J. Chem. Techn.* **2012**, *19*, 244–249. (b) Jeon, J. H.; Kim, J. T.; Kim, Y. J.; Kim, H. K.; Lee, H. S.; Kang, S. G.; Kim, S. J.; Lee, J. H. *Appl. Microbiol. Biotechnol.* **2009**, *81*, 865–874. (c) Bajpai D.; Tyagi V. *K. J. Oleo. Sci.* **2007**, *56*, 327–340.
- (24) (a) Spinella, S.; Ganesh, M.; Lo Re, G.; Zhang, S.; Raquez, J. M.; Dubois, P.; Gross, R. A. *Green Chem.* **2015**, *17*, 4146–4150. (b) Düşkünkörür, H. Ö.; Bégué, A.; Pollet, E.; Phalip, V.; Güvenilir, Y.; Avérous, L. *J. of Mol. Catal. B: Enzym.* **2015**, *115*, 20–28. (c) Yang, Y.; Zhang, J.; Wu, D.; Xing, Z.; Zhou, Y.; Shi, W.; Li, Q. *Biotechnol. Adv.* **2014**, *32*, 642–651. (d) Zhang, J.; Shi, H.; Wu, D.; Xing, Z.; Zhang, A.; Yang, Y.; Li, Q. *Process Biochem.* **2014**, *49*, 797–806.
- (25) (a) Aouf, C.; Lecomte, J.; Villeneuve, P.; Dubreucq, E.; Fulcrand, H. *Green Chem.* **2012**, *14*, 2328–2336. (b) Jiang, Z. *Biomacromolecules* **2011**, *12*, 1912–1919. (c) Masoumi, H. R.; Kassim, A.; Basri, M.; Abdullah, D. K. *Molecules* **2011**, *16*, 4672–4680. (d) Jadhav, S. R.; Vemula, P. K.; Kumar, R.; Raghavan, S. R.; John, G. *Angew. Chem. Int. Ed. Engl.* **2010**, *49*, 7695–7698.
- (26) (a) Poppe, J. K.; Fernandez-Lafuente, R.; Rodrigues, R. C.; Ayub, M. A. *Biotechnol. Adv.* **2015**, *33*, 511–525. (b) Kabbashi, N. A.; Mohammed, N. I.; Alam, M. Z.; Mirghani, M. E. S. *J. Mol. Catal. B: Enzym.* **2015**, *116*, 95–100. (c) Zhang, W.-W.; Yang, X.-L.; Jia, J.-Q.; Wang, N.; Hu, C.-L.; Yu, X.-Q. *J. Mol. Catal. B: Enzym.* **2015**, *115*, 83–89. (d) Liu, S.; Nie, K.; Zhang, X.; Wang, M.; Deng, L.; Ye, X.; Wang, F.; Tan, T. *J. Mol. Catal. B: Enzym.* **2014**, *99*, 43–50.

- (27) Franssen, M. C.; Steunenberg, P.; Scott, E. L.; Zuilhof, H.; Sanders, J. P. *Chem. Soc. Rev.* **2013**, *42*, 6491–533.
- (28) (a) Saranya, P.; Ramani, K.; Sekaran, G. *RSC Adv.* **2014**, *4*, 10680–10692. (b) Margesin, R.; Labbe, D.; Schinner, F.; Greer, C. W.; Whyte, L. G. *Appl. Environ. Microbiol.* **2003**, *69*, 3085–3092. (c) Margesin, R.; Zimmerbauer, G.; Schinner, F. *Biotechnol. Tech.* **1999**, *13*, 313–333.
- (29) Mita, L.; Sica, V.; Guida, M.; Nicolucci, C.; Grimaldi, T.; Caputo, L.; Bianco, M.; Rossi, S.; Bencivenga, U.; Eldin, M. S. M.; Tufano, M. A.; Mita, D. G.; Diano, N. *J. Mol. Catal. B: Enzym.* **2010**, *62*, 133–141.
- (30) (a) Samal, M.; Chercheja, S.; Rybacek, J.; Vacek Chocholousova, J.; Vacek, J.; Bednarova, L.; Saman, D.; Stara, I. G.; Stary, I. *J. Am. Chem. Soc.* **2015**, *137*, 8469–8474. (b) Lee, J.; Oh, Y.; Choi, Y. K.; Choi, E.; Kim, K.; Park, J.; Kim, M.-J. *ACS Catal.* **2015**, *5*, 683–689. (c) Lopez-Iglesias, M.; Busto, E.; Gotor, V.; Gotor-Fernandez, V. *J. Org. Chem.* **2015**, *80*, 3815–3824. (d) Rangel, H.; Carrillo-Morales, M.; Galindo, J. M.; Castillo, E.; Obregón-Zúñiga, A.; Juaristi, E.; Escalante, J. *Tetrahedron: Asymmetry* **2015**, *26*, 325–332.
- (31) (a) Toledo, M. V.; José, C.; Collins, S. E.; Ferreira, M. L.; Briand, L. E. *J. Mol. Catal. B: Enzym.* **2015**, *118*, 52–61. (b) Schär, A.; Nyström, L. *J. Mol. Catal. B: Enzym.* **2015**, *118*, 29–35. (c) Quintana, P. G.; Canet, A.; Marciello, M.; Valero, F.; Palomo, J. M.; Baldessari, A. *J. Mol. Catal. B: Enzym.* **2015**, *118*, 36–42. (d) Lopresto, C. G.; Calabrò, V.; Woodley, J. M.; Tufvesson, P. *J. Mol. Catal. B: Enzym.* **2014**, *110*, 64–71.

- (32) (a) Usui, K.; Yamamoto, K.; Shimizu, T.; Okazumi, M.; Mei, B.; Demizu, Y.; Kurihara, M.; Suemune, H. *J. Organic Chem.* **2015**, *80*, 6502–6508. (b) Rangel, H.; Carrillo-Morales, M.; Galindo, J. M.; Castillo, E.; Obregón-Zúñiga, A.; Juaristi, E.; Escalante, J. *Tetrahedron: Asymmetry* **2015**, *26*, 325–332. (c) Varga, A.; Naghi, M. A.; Füstös, M.; Katona, G.; Zaharia, V. *Tetrahedron: Asymmetry* **2014**, *25*, 298–304.
- (33) Lopez-Iglesias, M.; Busto, E.; Gotor, V.; Gotor-Fernandez, V. *J. Org. Chem.* **2012**, *77*, 8049–8055.
- (34) (a) Xia, B.; Li, Y.; Cheng, G.; Lin, X.; Wu, Q. *ChemCatChem* **2014**, *6*, 3448–3454. (b) Zheng, J.-Y.; Wang, Z.; Zhu, Q.; Zhang, Y.-J.; Yan, H.-D. *J. Mol. Catal. B: Enzym.* **2009**, *56*, 20–23.
- (35) (a) Moni, L.; Banfi, L.; Basso, A.; Carcone, L.; Rasparini, M.; Riva, R. *J. Org. Chem.* **2015**, *80*, 3411–3428. (b) Namiki, Y.; Fujii, T.; Nakada, M. *Tetrahedron: Asymmetry* **2014**, *25*, 718–724. (c) Moni, L.; Banfi, L.; Basso, A.; Galatini, A.; Spallarossa, M.; Riva, R. *The J. Org. Chem.* **2014**, *79*, 339–351. (d) Zheng, J.-Y.; Wang, S.-F.; Zhang, Y.-J.; Ying, X.-X.; Wang, Y.-g.; Wang, Z. *J. Mol. Catal. B: Enzym.* **2013**, *98*, 37–41. (e) Manzana Sapu, C.; Backvall, J. E.; Deska, J. *Angew. Chem.* **2011**, *50*, 9731–9734. (f) Garcia-Urdiales, E.; Alfonso, I.; Gotor, V. *Chem. Rev.* **2011**, *111*, PR110–PR180.
- (36) Méndez-Sánchez, D.; Ríos-Lombardía, N.; García-Granda, S.; Montejo-Bernardo, J.; Fernández-González, A.; Gotor, V.; Gotor-Fernández, V. *Tetrahedron: Asymmetry* **2014**, *25*, 381–386.

- (37) Rios-Lombardia, N.; Busto, E.; Gotor-Fernandez, V.; Gotor, V. *J. Org. Chem.* **2011**, *76*, 5709–5718.
- (38) (a) Szczesniak, P.; Pazdzierniok-Holewa, A.; Klimczak, U.; Stecko, S. *J. Org. Chem.* **2014**, *79*, 11700–11713. (b) Radu, A.; Moisă, M. E.; Toşa, M. I.; Dima, N.; Zaharia, V.; Irimie, F. D. *J. Mol. Catal. B: Enzym.* **2014**, *107*, 114–119. (c) Klossowski, S.; Brodzka, A.; Zysk, M.; Ostaszewski, R. *Tetrahedron: Asymmetry* **2014**, *25*, 435–442. (d) Brem, J.; Bencze, L.-C.; Liljebblad, A.; Turcu, M. C.; Paizs, C.; Irimie, F.-D.; Kanerva, L. T. *Eur. J. Org. Chem.* **2012**, 3288–3294.
- (39) Selvig, K.; Ruud-Christensen, M.; Aasen, A. J. *J. Med. Chem.* **26**, **1983**, 1514–1518.
- (40) Ruud-Christensen, M.; Salvesen, B. *J. Chromat.* **1984**, *303*, 433–435.
- (41) Rice, R. V.; Heights, H. *US. Patent* 2 715 125, 1955.
- (42) Chen, C. S.; Fujimoto, Y.; Girdaukas, G.; Sih, C. J. *J. Am. Chem. Soc.* **1982**, *104*, 7294–7299.
- (43) (a) Kitamoto, Y.; Kuruma, Y.; Suzuki, K.; Hattori, T. *J. Org. Chem.* **2015**, *80*, 521–527. (b) Petrenz, A.; María, P. D. d.; Ramanathan, A.; Hanefeld, U.; Ansorge-Schumacher, M. B.; Kara, S. *J. Mol. Catal. B: Enzym.* **2015**, *114*, 42–49. (c) Godoy, C. A.; Fernández-Lorente, G.; de las Rivas, B.; Filice, M.; Guisan, J. M.; Palomo, J. M. *J. Mol. Catal. B: Enzym.* **2011**, *70*, 144–148.

- (44) (a) Wikmark, Y.; Svedendahl Humble, M.; Bäckvall, J. E. *Angew. Chem. Int. Ed.* **2015**, *54*, 4284–4288. (b) Corici, L.; Pellis, A.; Ferrario, V.; Ebert, C.; Cantone, S.; Gardossi, L. *Adv. Synth. Catal.* **2015**, *357*, 1763–1774. (c) Ferrari, F.; Paris, C.; Maigret, B.; Bidouil, C.; Delaunay, S.; Humeau, C.; Chevalot, I. *J. Mol. Catal. B: Enzym.* **2014**, *101*, 122–132. (d) Escorcia, A. M.; Daza, M. C.; Doerr, M. *J. Mol. Catal. B: Enzym.* **2014**, *108*, 21–31. (e) Baum, I.; Elsässer, B.; Schwab, L. W.; Loos, K.; Fels, G. *ACS Catal.* **2011**, *1*, 323–336.
- (45) Trott, O.; Olson, A. J. *J. Comput. Chem.* **2010**, *31*, 455–461.
- (46) (a) Dodson, G. *Trends Biochem. Sci.* **1998**, *23*, 347–352. (b) Uppenberg, J.; Oehrner, N.; Norin, M.; Hult, K.; Kleywegt, G. J.; Patkar, S.; Waagen, V.; Anthonsen, T.; Jones, T. A. *Biochemistry* **1995**, *34*, 16838–16851. (c) Derewenda, Z. S.; Derewenda, U. *Biochem. Cell Biol.* **1991**, *69*, 842–851. (d) Brady, L.; Brzozowski, A. M.; Derewenda, Z. S.; Dodson, E.; Dodson, G.; Tolley, S.; Turkenburg, J. P.; Christiansen, L.; Huge-Jensen, B.; Norskov, L.; Thim, L.; Menge, U. *Nature* **1990**, *343*, 767–770.
- (47) Uppenberg, J.; Hansen, M. T.; Patkar, S.; Jones, T. A. *Structure* **1994**, *2*, 293–308.
- (48) Bradley, D.; Williams, G.; Lawton, M. *J. Org. Chem.* **2010**, *75*, 8351–8354.
- (49) Pettersen, E. F.; Goddard, T. D.; Huang, C. C.; Couch, G. S.; Greenblatt, D. M.; Meng, E. C.; Ferrin, T. E. *J. Comput. Chem.* **2004**, *25*, 1605–1612.
- (50) Sanner, M. F. *J. Mol. Graph. Model.* **1999**, *17*, 57–61.